Long-lasting Cadomian magmatic activity along an active northern Gondwana margin: U–Pb zircon and Sr–Nd isotopic evidence from the Brunovistulian Domain, eastern Bohemian Massif

Igor Soejono[1]*, Vojtěch Janoušek[1,2], Eliška Žáčková[1], Jiří Sláma[3], Jiří Konopásek[1,4], Matěj Machek[5], Pavel Hanžl[1]

[1] *Czech Geological Survey, Klárov 3, 118 21 Prague 1, Czech Republic*

[2] *Institute of Petrology and Structural Geology, Faculty of Science, Charles University, Albertov 6, 128 43 Prague 2, Czech Republic*

[3] *Institute of Geology of the CAS, v. v. i., Rozvojová 269, 165 00 Prague 6, Czech Republic*

[4] *Universitetet i Tromsø, Institutt for geologi, Postboks 6050 Langnes, 9037 Tromsø, Norway*

[5] *Institute of Geophysics of the CAS, v. v. i., Boční II-1401, 141 31 Prague 4, Czech Republic*

**Corresponding author (e-mail: igor.soejono@geology.cz, telephone: (+420)257089497, fax: (+420)257531376*

Keywords: Cadomian magmatic arc; Brunovistulian Domain; Bohemian Massif; Gondwana margin; U–Pb geochronology; Geochemistry

Running header: Long-lasting Cadomian magmatism in the eastern Bohemian Massif

Abstract

Cadomian magmatic complexes of the Brunovistulian Domain crop out in the eastern termination of the Bohemian Massif. However, the age, nature and geotectonic affinity of some of pre-Variscan (meta-)igneous rock complexes from this domain are still unknown. Geochronological and geochemical study of the granitic rocks across the Brunovistulian Domain reveals new information about the timing and nature of this magmatic activity originally situated along the northern margin of Gondwana. Zircon U–Pb data (601 ± 3 Ma, Brno Massif ; 634 ± 6 Ma, paraautochtonous core of the Svratka Dome; 568 ± 3 Ma, Bíteš orthogneiss from the allochtonous Moravicum indicate the prolonged magmatic activity within the Brunovistulian Domain during the Ediacaran. The major- and trace-element and Sr–Nd isotopic signatures show heterogeneous geochemical characteristics of the granitic rocks and suggest a magmatic-arc geotectonic setting. The two-stage Depleted Mantle Nd model ages (*c*. 1.3–2.0 Ga) indicate derivation of the granitic rocks from a relatively primitive crustal source, as well as from an ancient and evolved continental crust of the Brunovistulian Domain.

These results constrain the magmatic-arc activity to *c.* 635–570 Ma and provide a further evidence for a long-lived (at least *c*. 65 Myr) and likely episodic subduction-related magmatism at the northern margin of Gondwana. The presence of granitic intrusions derived from variously mature crustal sources at different times suggests heterogeneous crustal segments to having been involved in the magmatic-arc system during its multi-stage evolution.

Introduction

The Variscan orogenic belt in Europe incorporates many of Cadomian magmatic complexes produced by the Late Proterozoic–Cambrian igneous activity. The widespread and voluminous arc-related magmatism was originally situated along the Andean-type active margin of the Gondwana supercontinent and represents an important episode of crustal growth within Europe and Western Asia (Nance et al. 1991, 2002; Murphy et al. 2002; von Raumer et al. 2002; Pereira et al. 2011). Continental segments of the Cadomian belt including the magmatic arc (Nance et al. 1991, 2002; Murphy et al. 2004) rifted off the northern Gondwana margin during the Early Palaeozoic (Nance et al. 1991, 2010; Kemnitz et al. 2002; Linnemann et al. 2008) and subsequently accreted to Laurussia during the Variscan Orogeny (Franke 2000; Winchester et al. 2002). The overall extent and duration of the Cadomian magmatic-arc activity is constrained, from localities scattered through the Variscan belt, to be Neoproterozoic–Early Cambrian (Nance et al. 1991; von Raumer et al. 2002; Murphy et al. 2004; Linnemann et al. 2008).

Arc-related magmatic suites have been extensively reported from the Cadomian basement in the Teplá–Barrandian Unit (Mašek and Zoubek 1980; Zulauf et al. 1997; Dörr et al. 1998, 2002; Sláma et al. 2008a; Hajná et al. 2010, 2013; Drost et al. 2011) and the Saxothuringian Domain (Linnemann and Romer 2002; Linnemann et al. 2014) of the Bohemian Massif, Iberian Massif (Fernández-Suárez et al. 2000; Bandres et al. 2002; Albert et al. 2015a, b; Rubio-Ordóñez et al. 2015), the Eastern Pyrenees (Castiñeiras et al. 2008; Casas et al. 2015), the Armorican Massif (D’Lemos et al. 1990; Strachan et al. 1996; Chantraine et al. 2001; Gerdes and Zeh 2006), the Alps (Schaltegger et al. 1997; Neubauer et al. 2002; Schulz et al. 2004), the Tauride–Anatolide Platform (Ustaömer et al. 2005; Gürsu and Conczoglu 2008; Şahin et al. 2014) and the Central Iranian Block (Moghadam et al. 2015).

The Brunovistulian Domain of the Bohemian Massif is generally assumed to be a continental segment derived from the northern Gondwana margin (Dudek 1980; Finger et al.

2000a; Kalvoda et al. 2008). From the Late Devonian to Carboniferous (*i.e.* Variscan), the Brunovistulian Domain was incorporated into the collision zone between Laurussia and peri-Gondwana microcontinents (Matte et al. 1990; Franke 2000; Winchester et al. 2002; Schulmann et al. 2009). Despite relatively well-constrained Cadomian formation of the Brunovistulian Domain, the age, nature and geotectonic affinity of some bodies of pre-Variscan (meta-)igneous rocks are still unknown, because of the scarcity of modern geochronological and isotopic data from this area.

The aim of this paper is to present new U–Pb zircon ages of (meta-)granitic rocks from three key parts of the Brunovistulian Domain in the south-western Moravia. The results of the geochronological study are combined with Sr–Nd isotopic signatures and whole-rock geochemistry. The newly acquired results are compared with previously published geochronological and geochemical data from the Brunovistulian Domain in order to provide better insight into the pre-collisional (pre-Variscan) evolution of the crystalline basement in the easternmost part of the Variscan orogenic belt.

Geological setting

The eastern part of the Bohemian Massif (Fig. 1a, b) is traditionally subdivided into two domains. The medium-grade Brunovistulian Domain (Suess 1926; Dudek 1980; Schulmann et al. 1991, 1994; Kalvoda et al. 2008) in the east was underthrust beneath the high-grade Moldanubian Domain to the west (Suess 1912; Dallmeyer et al. 1995; Franke 2000; Schulmann et al. 2009) (Fig. 1b, c, 2).

Derivation of the Brunovistulian Domain from the northern margin of Gondwana is generally accepted (Matte et al. 1990; Finger et al. 1995, 2000a; Friedl et al. 2000), but its exact provenance remains controversial. The Brunovistulian Domain is mostly considered as a continental segment of Avalonian (South American) affinity (Moczydlowska 1997; Tait et al. 1997; Finger et al. 2000a; Friedl et al. 2000; Mazur et al. 2010) merged together with the

Moldanubian Domain during the Variscan collision. In contrast, several authors rather suggested that it had a peri-Baltic affinity (Belka et al. 2002; Vavrdová et al. 2003; Kalvoda et al. 2002, 2008; Nawrocki et al. 2004). The thrust boundary between the Moldanubian and Brunovistulian domains is mostly assumed to be a remnant of an Early Palaeozoic ocean (Höck et al. 1997; Finger et al. 1998) representing a southward curved continuation of the Rheic suture (Finger et al. 1998; Murphy et al. 2006; Linnemann et al. 2008; von Raumer and Stampfli 2008; Nance et al. 2010; Mazur et al. 2012) that can be traced further to the west along the European Variscan belt. Some studies suggested a subduction zone to have been located between the Moldanubian and the Brunovistulian domains (Matte et al. 1990; Höck et al. 1997; Franke 2000; Konopásek et al. 2002; Finger et al. 2007) at least during the early Variscan evolution. However, Schulmann et al. (2009, 2014) and Košler et al. (2014) proposed a different idea, namely that the Moldanubian Domain represents just a rifted and thinned marginal part of the Brunovistulian continental segment. This concept assumes that these units were never separated by a large-scale oceanic domain and that the formation of the Moldanubian Domain took place during the Early Palaeozoic and subsequent Variscan orogenic evolution.

The Brunovistulian Domain itself is further subdivided into the Brunovistulicum *sensu stricto (s.s.),* and the Moravicum (continuing as a Silesicum to the north; Hanžl et al. 2007b and references therein) (Fig. 1b, c, 2), which differ from each other mainly in the degree of the Variscan reworking. The strong Variscan deformation largely overprinted the primary depositional/emplacement structures in these units and their mutual pre-Variscan position remains a matter of discussion. During the Variscan Orogeny, the Moravicum nappe system was thrust over the Brunovistulicum *s.s.* from the west (Suess 1912, 1926; Dudek 1980; Schulmann et al. 1991). Moreover, most of the Brunovistulicum *s.s.* is covered by the Devonian sedimentary rocks, the Variscan flysch sequences and the Cretaceous–Paleogene sedimentary rocks of the Outer Carpathians from the East (Dudek 1980; Jelínek and Dudek 1993; Hladil et al. 1999).

The exposed parts of the Brunovistulicum *s.s.* are dominantly represented by the magmatic rocks of the Brno and the Thaya (Dyje) massifs (Suess 1912; Dudek 1980; Finger et al. 1995, 2000a; Leichmann and Höck 2008) and by paraautochtonous metagranite body located in the footwall of the Moravicum (the core of the Svratka Dome) (Fig. 1c, 2). Relicts of their host pre-Cadomian basement (Dudek et al. 1980; Fritz et al. 1996) are preserved as blocks of gneisses and migmatites.

The Brno Massif has been interpreted as a Cadomian rock assemblage built by the Western and Eastern granitoid complexes (*e.g.*, Finger and Pin 1997; Hanžl and Melichar 1997) and by a relict of ocean domain (the Central Basic Belt) sandwiched in between them (Hanžl and Melichar 1997; Finger et al. 2000a, b; Leichmann and Höck 2008) (Fig. 1c, 2). The Western Granitoid Complex consists of granites, granodiorites, diorites and also abundant blocks of thermally affected host-rocks, whereas the Eastern Granitoid Complex is built mainly by granodiorites, tonalities and quartz diorites. The Central Basic Belt contains low-grade metamorphosed mafic plutonic and volcanic rocks.

The granitoids of the Thaya Massif are assumed to be a south-western continuation of the Western Granitoid Complex of the Brno Massif (Finger et al. 1995, 2000a; Leichmann and Höck 2008) off-set by the marginal fault of the Permian Boskovice Basin.

The core of the Svratka Dome is made up by a paraautochtonous metagranite body (Souček et al. 1992; Hanžl et al. 2007a). Low-grade metamorphosed Devonian siliciclastic sediments and limestones (Hladil et al. 1999) are incorporated within the metagranites as narrow tectonic slices close to the overthrust Moravian nappes.

The rock association of the Brunovistulicum *s.s.* is generally considered as a product of a subduction-related magmatism (Jelínek and Dudek 1993; Finger and Pin 1997). The Eastern

Granitoid Complex has been interpreted as a result of a primitive arc-related magmatism, whereas the Western Granitoid Complex was more likely produced by melting of a pre-existing continental crust (Hanžl and Melichar 1997; Finger et al. 2000a).

For the Central Basic Belt, a minimum age of 725 ± 15 Ma was proposed based on the Pb–Pb zircon evaporation data from associated rhyolites (Finger et al. 2000b).

The Neoproterozoic intrusion of the Brno Massif granitoids is documented by the U–Pb zircon age of 584 ± 5 Ma from the Western Granitoid Complex diorite (van Breemen et al. 1982) as well as by the $^{40}Ar/^{39}Ar$ cooling ages of amphiboles (586.9 ± 0.5 Ma from Eastern Granitoid Complex and 596.9 ± 2.1 Ma from the Western Granitoid Complex diorites) (Fritz et al. 1996). The metagranite from the Thaya Massif provided a Late Neoproterozoic U–Pb zircon age of 575 ± 2 Ma (Friedl et al. 2004) and Rb–Sr whole-rock age of 551± 6 Ma (Scharbert and Batík 1980).

The Moravicum constitutes a north–south elongated belt (Fig. 1c, 2) of deformed and metamorphosed rocks. It is represented by the Svratka Dome and the Thaya (Dyje) Dome anticlinal structures, forming tectonic windows (Suess 1912), and the Letovice Complex (Höck et al. 1997; Soejono et al. 2010). The Moravicum, separated from the Moldanubian Domain by the Micaschist Zone (Suess 1912), has been traditionally considered as a deformed margin of the Brunovistulicum (Dudek 1980; Schulmann et al. 1991). Other workers (*e.g.*, Winchester et al. 2006) proposed that the Moravicum is an independent fragment of the Avalonian crust sandwiched between the strongly deformed and metamorphosed Moldanubian Domain in the west and relatively undeformed rocks of the Brunovistulicum *s. s.* in the east. The Moravicum was affected by the Variscan Barrovian-type metamorphism (Höck 1995; Štípská and Schulmann 1995; Štípská et al. 2015), where the metamorphic inversion was caused by imbrication of crustal nappes (Suess 1912; Štípská and Schulmann 1995).

The Svratka and Thaya domes are made up by an assemblage of orthogneiss (Bíteš orthogneiss in the Svratka Dome, Bíteš and Weitersfeld orthogneisses in the Thaya Dome) and metapelite nappes (Dudek 1980; Schulmann et al. 1991; Štípská and Schulmann 1995) thrust over the Brunovistulian basement (Fig. 1c, 2). The U–Pb zircon ages of *c*. 580 Ma from the Bíteš orthogneiss (Friedl et al. 2000, 2004) and matching $^{40}Ar/^{39}Ar$ hornblende cooling age of 575.6 ± 2.2 Ma from associated amphibolite (Fritz et al. 1996) confirm its Cadomian protolith age. The Letovice Complex is formed mainly by amphibolites and metagabbros interpreted as a relict of an Early Cambrian (*c*. 530 Ma) incipient oceanic basin located between the Brunovistulian and the Moldanubian domains incorporated into the Variscan thrust-nappe system of the Moravicum (Soejono et al. 2010) (Fig. 1c, 2).

Sample descriptions

The sampling was focused on regionally important (meta-)igneous bodies within the Brunovistulian Domain in the south-western Moravia (Fig. 1c). Our aim was to constrain their intrusive ages, ages of inherited zircons and whole-rock geochemical characteristics. Samples UD 3 and UD 5 were collected from the Brunovistulicum *s.s*. and sample UD 2 from the Moravicum.

Biotite–amphibole granodiorite UD 3, from the abandoned quarry Anenský mlýn (WGS84 coordinates: N 49° 08.103', E 16° 31.906'), is a characteristic rock of the Western Granitoid Complex of the Brno Massif. The granodiorite encloses abundant fine-grained mafic enclaves of variable size and shape that display mixing/mingling textures. The sample UD 3 is medium-grained, weakly porphyritic and exhibits a random or locally weak magmatic fabric defined by the preferred orientation of K-feldspar phenocrysts (Fig. 3a). The granodiorite UD 3 consists of the biotite–amphibole–plagioclase–K-feldspar–quartz mineral assemblage. Biotite and amphibole are locally chloritized and plagioclase is partly sericitized (Fig. 3b). Accessory zircon, apatite and opaque minerals are also present.

Strongly deformed metagranite UD 5 was collected from the core of the Svratka tectonic window south of Dolní Loučky (WGS84 coordinates: N 49° 21.405', E 16° 21.795'), and represents granitoids of the Brunovistulian basement in the tectonic footwall of the Moravicum nappe system. This fine-grained metagranite has only locally preserved igneous texture and generally shows well-developed anastomosing solid-state foliation (Fig. 3c). The metagranite UD 5 consists of mostly recrystallized quartz, K-feldspar and plagioclase with fine-grained muscovite, scarce biotite and chlorite (Fig. 3d). Accessory minerals are zircon, apatite and carbonate.

Sample UD 2 of the Bíteš orthogneiss from the vicinity of Štěpánov nad Svratkou (WGS84 coordinates: N 49° 30.143', E 16° 21.611'), represents typical meta-granitic lithology of the Moravicum. The orthogneiss UD 2 is made mainly of quartz accompanied by the mineral assemblage plagioclase–K-feldspar–muscovite–clinozoisite and small amount of biotite (Fig. 3e, f). Opaque mineral, apatite and zircon are the main accessories. Quartz and feldspars are often recrystallized and feldspars replaced by sericite. The sample UD 2 shows fine- to medium-grained porphyroclastic texture (Fig. 3e) and is characterized by a subhorizontal high-grade foliation defined by alternation of recrystallized polymineralic plagioclase–K-feldspar and quartz domains separated by bands of muscovite and biotite (Fig. 3f).

Analytical techniques

Whole-rock geochemistry

The whole-rock major- and trace-element analyses of magmatic rocks were determined in the Acme Analytical Laboratories Ltd., Vancouver, by Inductively-Coupled Plasma Mass Spectrometry (ICP–MS). Total abundances of the major- and minor-element oxides (‘Group 4A’) were determined by ICP-Emission Spectrometry (ICP-OES) following a $LiBO_2/Li_2B_4O_7$ fusion and dilute nitric digestion. Loss on ignition (LOI) was obtained by weigh difference after heating to 1000 °C. The detection limits are 0.01 wt. % for most of the oxides, except

Fe_2O_3 (0.04 %), P_2O_5 (0.001 %) and Cr_2O_3 (0.002 %). Rare earth and refractory elements were determined by ICP-Mass Spectrometry (ICP-MS) following a $LiBO_2/Li_2B_4O_7$ fusion and nitric acid digestion of a 0.2 g sample ('Group 4B'). In addition a separate 0.5 g split was digested in Aqua Regia and analysed by ICP-MS to report the precious and base metals (Pb, Ni, Zn and Cu, 'Group 1DX'). See *http://www.acmelab.com* for details of the analytical procedure and respective detection limits. Data management, recalculation, and plotting of the whole-rock geochemical data were facilitated using *GCDkit* (Janoušek et al. 2006).

Strontium–neodymium isotopic compositions

For the radiogenic isotope determinations, samples were dissolved using a combined HF–HCl–HNO_3 digestion. Strontium and bulk REE were isolated by exchange chromatography techniques following the procedure of Pin et al. (1994) (PP columns filled with Sr. spec and TRU. spec Eichrom resins, respectively). The Nd was further separated from the REE fraction on PP columns with Ln. spec Eichrom resin (Pin and Zalduegui 1997). Complete analytical details were reported by Míková and Denková (2007).

Isotopic analyses were performed on a Finnigan MAT 262 thermal ionization mass spectrometer housed at the Czech Geological Survey in dynamic mode using a single Re filament with Ta addition for Sr measurement and double Re filament assembly for Nd. The $^{143}Nd/^{144}Nd$ ratios were corrected for mass fractionation to $^{146}Nd/^{144}Nd = 0.7219$ (Wasserburg et al. 1981), $^{87}Sr/^{86}Sr$ ratios assuming $^{86}Sr/^{88}Sr = 0.1194$. External reproducibility was estimated from repeat analyses of the BCR-1 ($^{143}Nd/^{144}Nd = 0.512621 \pm 20$ (2σ, n = 5) and NBS 987 ($^{87}Sr/^{86}Sr = 0.710248 \pm 28$ (2σ), n = 10) isotopic standards. The Rb, Sr, Sm and Nd concentrations were obtained by ICP-MS in Acme Laboratories (see above).

The decay constants applied to age-correct the isotopic ratios are from Steiger and Jäger (1977: Sr) and Lugmair and Marti (1978: Nd). The ε^i_{Nd} values were obtained using Bulk Earth parameters of Jacobsen and Wasserburg (1980) ($^{147}Sm/^{144}Nd_{CHUR} = 0.1967$ and present-day $^{143}Nd/^{144}Nd_{CHUR}$ = 0.512638), the two-stage Depleted Mantle Nd model ages (T_{Nd}^{DM}) were calculated after Liew and Hofmann (1988) ($^{147}Sm/^{144}Nd_{DM}$ = 0.219, present-day $^{143}Nd/^{144}Nd_{DM}$ = 0.513151, average crustal $^{147}Sm/^{144}Nd_{CC}$ = 0.12).

Laser ablation ICP-MS U–Pb zircon dating

About twenty kilograms of the fresh rock were crushed, sieved, and zircon grains were separated from the samples using the Wilfley shaking table and heavy liquids, mounted in epoxy-filled blocks and polished. Zoning patterns in individual grains were observed, and presence of older inherited components checked, by cathodoluminescence detector mounted on the electron microprobe at the Institute of Petrology and Structural Geology, Charles University in Prague.

The U–Pb and Pb–Pb zircon ages were obtained using two different laser-ablation (LA) ICP-MS analytical protocols at the University of Bergen, Norway:

a) Isotopic analysis of zircon by laser ablation ICP-MS followed the technique described in Košler et al. (2002) and Košler and Sylvester (2003). A Thermo-Finnigan Element 2 sector field ICP-MS coupled to a 213 nm solid state Nd-YAG laser (NewWave UP213) at Bergen University, Norway, was used to measure Pb/U and Pb isotopic ratios in zircons. The sample introduction system was modified to enable simultaneous nebulisation of a tracer solution and laser ablation of the solid sample (Horn et al. 2000). Natural Tl ($^{205}Tl/^{203}Tl$ = 2.3871; Dunstan et al. 1980), ^{209}Bi and enriched ^{233}U and ^{237}Np (>99%) were used in the tracer solution, which was aspirated to the plasma in an argon–helium carrier gas mixture through an Apex desolvation nebuliser (Elemental Scientific) and a T-piece tube attached to the back end of the plasma torch. A helium gas line carrying the sample from the laser cell to the plasma was also attached to the T-piece tube. The laser was fired at a repetition rate of 5 Hz and energy of 80 mJ. Linear laser rasters (30–100 microns) were produced by repeated scanning of the laser beam at a speed of 10 microns/second across the zircon sample surface. Typical acquisitions consisted of 40 second measurement of blank followed by measurement of U and Pb signals from the ablated zircon for another 110 seconds. The data were acquired in time resolved – peak jumping – pulse counting mode with 1 point measured per peak for masses 202 (flyback), 203 (Tl), 204 (Pb), 205 (Tl), 206 and 207 (Pb), 209 (Bi), 233 (U), 237 (Np), 238 (U), 249 (^{233}U oxide), 253 (^{237}Np oxide) and 254 (^{238}U oxide). Raw data were corrected for dead time of the electron multiplier and processed offline in a spreadsheet-based program (Lamdate; Košler et al. 2002). Data reduction included correction for gas blank, laser-induced elemental fractionation of Pb and U and instrument mass bias. Minor formation of oxides of U and Np was corrected for by adding signal intensities at masses 249, 253 and 254 to the intensities at masses 233, 237 and 238, respectively. No common Pb correction was applied to the data but the low concentrations of common Pb were checked by observing ^{206}Pb/^{204}Pb ratio during measurements. Residual elemental fractionation and instrumental mass bias were corrected by normalization to the natural zircon reference material GJ-1 (Jackson et al. 2004). Zircon reference material 91500 (Wiedenbeck et al. 1995) was periodically analysed during the measurement for quality control and the obtained mean value of 1065 ± 5 (2σ) Ma corresponds with the published reference value of *c.* 1065 Ma (Wiedenbeck et al. 1995).

b) A Nu AttoM high resolution ICP-MS coupled to a 193 nm ArF excimer laser (Resonetics RESOlution M-50 LR) at Bergen University, Norway, was used to measure the Pb/U and Pb isotopic ratios in zircons. The laser was fired at a repetition rate of 5 Hz and energy of 80 mJ with 19 microns spot size. Typical acquisitions consisted of 15 second measurement of blank followed by measurement of U and Pb signals from the ablated zircon for another 30 seconds. The data were acquired in time resolved – peak jumping – pulse counting mode with 1 point measured per peak for masses ^{204}Pb + Hg, ^{206}Pb, ^{207}Pb, ^{208}Pb, ^{232}Th, ^{235}U, and ^{238}U. Due to a non-linear transition between the counting and attenuated (= analogue) acquisition modes of the ICP instruments, the raw data were pre-processed using a purpose-made Excel macro. As a result, the intensities of ^{238}U are left unchanged if measured in a counting mode and recalculated from ^{235}U intensities if the ^{238}U was acquired in an attenuated mode. Data reduction was then carried out off-line using the Iolite data reduction package version 3.0 with VizualAge utility (Petrus and Kamber 2012). Full details of the data reduction methodology can be found in Paton et al. (2010). The data reduction included correction for gas blank, laser-induced elemental fractionation of Pb and U and instrument mass bias. For the data presented here, blank intensities and instrumental bias were interpolated using an automatic spline function while down-hole inter-element fractionation was corrected using an exponential function. No common Pb correction was applied to the data but the low concentrations of common Pb were checked by observing $^{206}Pb/^{204}Pb$ ratio during measurements. Residual elemental fractionation and instrumental mass bias were corrected by normalization to the natural zircon reference material Plešovice (Sláma et al. 2008b). Zircon reference materials GJ-1 (Jackson et al. 2004) and 91500 (Wiedenbeck et al., 1995) were periodically analysed during the measurement for quality control and the obtained mean values of 599.9 ± 2.1 (2σ) Ma and 1063.0 ± 3.2 (2σ) Ma are accurate within the published reference values (600.5 ± 0.4 Ma, Schaltegger et al. 2015; 1065 Ma, Wiedenbeck et al. 1995, respectively). The zircon U–Pb ages are presented as concordia diagrams generated with the ISOPLOT program v. 3.6 (Ludwig 2008).

Results

Whole-rock geochemistry

The geochemical data from the samples UD 3, UD 5 and UD 2 were compared with previously published chemical analyses of granitic rocks from the Western and Eastern granitoid complexes of the Brno Massif (Hanžl and Melichar 1997; Leichmann and Höck 2008), as well as metagranites and mylonites from the paraautochtonous basement of the

Svratka Dome and the Bíteš orthogneiss nappe (Moravicum) (Souček et al. 1992; Hanžl et al. 2007a).

Major elements

The three studied samples are subalkaline granites to granodiorites as demonstrated by the multielement R_1–R_2 plot (De La Roche et al. 1980) (Fig. 4a) as well as by the Total Alkalis–Silica (TAS) diagram (Cox et al. 1979) (Fig. 4b). Both metagranite UD 5 and orthogneiss UD 2 are moderately peraluminous (A/CNK = 1.12, Table 1) in contrast to subaluminous (A/CNK = 1.04) granodiorite from the Brno Massif. This is also documented by the multielement B–A diagram (Debon and Le Fort 1983) modified by Villaseca et al. (1998) (Fig. 4c). In the binary SiO_2–K_2O plot (Peccerillo and Taylor 1976) (Fig. 4d), the samples UD 5 and UD 2 classify as (normal-K) calc-alkaline to high-K calc-alkaline, while the Brno Massif granodiorite (UD 3) is distinctly potassic. In all four classification diagrams the newly analyzed samples fall close to the fields defined by the previously published compositions of the Western Granitoid Complex and Moravicum orthogneisses, as appropriate. The only exception is the granodiorite sample (UD 3) being enriched in K_2O in the SiO_2–K_2O plot (Fig. 4d).

Major-element composition of all three new samples is silicic (SiO_2 = 69.2–71.6 wt. %) (Fig. 5) with variable K_2O/Na_2O ratio ranging from 0.71 in orthogneiss (UD 2) through 1.33 of metagranite (UD 5) to 1.55 in relatively potassic granodiorite (UD 3). The major-element compositions of all three new samples plot within the compositional range of the Brno Massif granitoids, metagranites and mylonites of the Svratka Dome core and the Bíteš orthogneisses. They often show a negative correlation of SiO_2 with major- and minor-element oxides (TiO_2, Al_2O_3, FeOt, MgO and CaO).

Trace elements

The trace-element patterns, in spider plot normalized by average composition of the upper continental crust (Taylor and McLennan 1995), are very similar to each other and show mostly trends close to the upper crustal average, with distinct troughs it Th, U, Nb, and Ta and perceptible depletion in HREE (Fig. 6a). All three samples are also depleted in P; the orthogneiss UD 2 shows in addition spikes in Ba and Sr.

Chondrite-normalized (Boynton 1984) REE patterns (Fig. 6b) are also very similar in all three samples, featuring moderate enrichment in LREE (La_N/Yb_N = 15.3–44.3, La_N/Sm_N = 4.5–10.4; Table 2) with weak depletion in HREE. Typical of metagranite UD 5 and orthogneiss UD 2 are weak negative Eu anomalies (Eu/Eu* = 0.59 and 0.84, respectively), while the Brno Massif granodiorite UD 3 displays a distinctly positive one (Eu/Eu* = 1.26), perhaps reflecting feldspar(s) accumulation.

Both types of multielement patterns for the studied samples best fit within the variability of Moravicum orthogneisses, but also within the Western Brno Massif granodiorites (Fig. 6).

In addition, the Zr concentrations in all three samples were used to determine zircon saturation temperatures (Watson and Harrison 1983), which should provide a maximum constraint upon the magma temperature. The calculated temperatures are 825 °C for granodiorite UD 3, 760 °C for the protolith of the metagranite UD 5 and 749 °C for the protolith of the orthogneiss UD 2.

Sr–Nd isotopic data

The Sr–Nd isotopic compositions of the three samples, both raw and age-corrected to their respective intrusive ages, are summarized in the Table 3. The Sr–Nd isotopic composition of the Western Brno Massif granodiorite UD 3 is the most primitive, close to the Bulk Earth ($^{87}Sr/^{86}Sr_i$ = 0.7048; ε^i_{Nd} = –1.0). The Bíteš orthogneiss UD 2 on the other hand reflects a generation from a mature crustal source ($^{87}Sr/^{86}Sr_i$ = 0.7101; ε^i_{Nd} = –10.0); the paraautochtonous metagranite UD 5 falls between these two extremes ($^{87}Sr/^{86}Sr_i$ = 0.7052; ε^i_{Nd} = –3.7). The variability in the Nd isotopic compositions is directly reflected by the two-stage Depleted Mantle Nd model ages (T_{Nd}^{DM}) (granodiorite UD 3: 1.33 Ga, metagranite UD 5: 1.57 Ga, Bíteš orthogneiss UD 2: 2.01 Ga).

Laser ablation ICP-MS U–Pb zircon dating

Three samples (UD 3, UD 5, UD 2) from the main parts of the Brunovistulian Domain were dated using LA-ICP-MS U–Pb method on zircon. Isotopic data with corresponding ages are given in Online Resource. The oscillatory zoning observed in cathodoluminescence (CL) images of zircon grains from all samples (Fig. 7) corresponds to the crystallization from melt.

The zircon grains from the granodiorite of the Brno Massif (UD 3) are transparent, pale brown to colourless and generally have long-prismatic habitus. In CL images, most grains are euhedral and oscillatory zoned (Fig. 7a). A total of 44 analyses were performed in the sample UD 3, of which 31 were used. Dating of sample UD 3 yielded a concordia age of 601 ± 3 Ma (2σ, Fig. 8a), interpreted as the Late Proterozoic intrusive age of the granodiorite. No inherited zircon cores were either observed in CL images or were detected by the LA-ICP-MS analyses.

Zircon population from the metagranite UD 5 (the Brunovistulian basement in the core of the Svratka Dome) is heterogeneous and consists of pale brown to light pink, euhedral and/or subhedral grains. Cathodoluminescence images show mostly euhedral oscillatory growth zoning and infrequent inherited cores (Fig. 7b). From sample UD 5, 19 analyses were performed, of which only 11 were concordant. These concordant analyses combine into a concordia age of 634 ± 6 Ma (2σ, Fig. 8b), interpreted as the magmatic crystallization age of this metagranite. The single analysis of *c*. 1670 Ma is interpreted as a xenocrystic core while the detection of one c. 400 Ma zircon most probably reflects Pb loss during metamorphism.

Zircon population of the Bíteš orthogneiss UD 2 (Moravicum’s nappe) contains generally prismatic, euhedral, colourless to pale pink grains, mostly with oscillatory zoning. Corroded and rounded inherited cores are very common (Fig. 7c). CL-bright outer rims, possibly related to a recrystallization or new zircon growth, were also found in some of the grains (Fig. 7c). However, their rims were too thin to be dated by LA-ICP-MS. A total of 76 analyses were performed in the sample UD 2, of which 74 were used. Analyses placed outside the cores combine into a concordia age of 568 ± 3 Ma (2σ, Fig. 8c), interpreted as the Late Proterozoic crystallization age of the Bíteš orthogneiss magmatic protolith. Dating of the frequent inherited cores shows a range of ages between *c*. 1.1 and 2.1 Ga and two dates at *c*. 2.5 Ga and *c*. 2.7 Ga (Fig. 9).

Discussion

Age of Cadomian magmatism in the Brunovistulian Domain

The new LA-ICP-MS U–Pb zircon age of 601 ± 3 Ma for the Western Granitoid Complex of the Brno Massif (granodiorite UD 3) is significantly older than the conventional U–Pb zircon age of 584 ± 5 Ma for a diorite of the same geological unit dated by van Breemen et al. (1982). The Ar–Ar hornblende dating of the Eastern Granitoid Complex diorite (south of Blansko) also gave a younger age of 586.9 ± 0.5 Ma (Fritz et al. 1996) as did the metagranite from the Thaya Massif (575 ± 2 Ma: U–Pb zircon age of Friedl et al. 2004). On the other hand, our age agrees remarkably well with the Ar–Ar hornblende age of 596.9 ± 2.1 Ma obtained from a diorite, also from the UD 3 locality (Anenský mlýn quarry), by Fritz et al. (1996), indicating a relatively rapid cooling.

The new 634 ± 6 Ma LA-ICP-MS U–Pb zircon age for the metagranite UD 5 represents both the first available geochronological datum from the paraautochton in the core of the Svratka Dome and also the oldest yet known intrusive age for granitoids of the Brunovistulicum *s.s*.

The protolith of the Bíteš orthogneiss UD 2 from the allochtonous Moravicum has also Late Proterozoic, albeit significantly younger, intrusive age of 568 ± 3 Ma that correlates well with the U–Pb ages reported from the Moravicum and the Silesian Domain (van Breemen et al. 1982; Friedl et al. 2000, 2004; Kröner et al. 2000; Oberc-Dziedzic et al. 2003; Mazur et al. 2010, 2012), the Teplá–Barrandian Unit (Dörr et al. 2002; Hajná et al. 2013) as well as from the Saxothuringian Domain (Linnemann et al. 2014).

Taken together, our new *in situ* U–Pb zircon data confirm the generally held idea of Cadomian origin of the Brunovistulian Domain (Dudek 1980; Finger et al. 2000a; Leichmann and Höck 2008). In particular, they bring further evidence for a long-lived Late Proterozoic (Ediacaran) arc-related magmatic activity within the Brunovistulian Domain (at least *c.* 635–575 Ma). This is largely in line with the published 630–530 Ma K–Ar cooling ages (Dudek and Melková 1975; recalculated to the new K decay constants of Steiger and Jäger 1977) of the samples from deep boreholes drilled into the eastern part of the Brunovistulian Domain concealed under the sediments of the Carpathian Foredeep in SE Moravia.

Prospective sources of the Cadomian magmas

The studied (meta-)granitic rocks, and literature data from the same units, show major- and trace-element characteristics resembling calc-alkaline, continental magmatic arc-related granites (Fig. 10). However, new whole-rock geochemical and Sr–Nd isotopic signatures provide an evidence that the granodiorite UD 3 of the western part of the Brno Massif and the metagranite UD 5 from the footwall of the Moravicum (Brunovistulicum *s.s.*) originated by partial melting of a geochemically less evolved source, whereas the orthogneiss UD 2 of the Moravicum was generated from an ancient, mature crustal segment.

By their chemistry, the samples from the Brunovistulicum *s.s.* (UD 3 and UD 5) resemble I- or transitional I/S-type granite suites. Most typically, the sample UD 3 is subaluminous, less siliceous (granodioritic) and thus falling into the field of low-peraluminous granites in Fig. 4c. Moreover, it is depleted in Th, U, Nb and Ta if compared with typical upper crustal compositions (Fig. 6a). Its Sr–Nd isotopic composition is the most primitive of the studied samples, close to the Bulk Earth ($^{87}Sr/^{86}Sr_i$ = 0.705; ε^{i}_{Nd} = –1.0). It falls just at the least evolved limit of the Sr–Nd isotopic data ($^{87}Sr/^{86}Sr_i$ = 0.705–0.710; ε_{Nd}^{i} = –1.0 to –7.0) from the Western Granitoid Complex (aka Thaya Terrane) of Finger and Pin (1997). The neodymium in the paraautochthonous metagranite UD 5 is somewhat less radiogenic ($^{87}Sr/^{86}Sr_i$ = 0.705; ε_{Nd}^{i} = –3.7).

Still, the most characteristic features of the Western Granitoid Complex are the Sr–Nd isotopic compositions at the other end of the spectrum, resembling mature continental crust (Finger et al. 2000a). Based on these observations, as well as on elevated silica and potassium contents, the same authors assumed mostly metasedimentary source of the granitic magmas, with only limited participation of the juvenile lower crustal lithologies or mantle-derived magmas. The latter notion is also supported by field observations of mingling between mafic and felsic magmas in the Anenský mlýn quarry (UD 3).

The rather evolved chemistry of the Western Granitoid Complex contrasts with the much more primitive Sr–Nd isotopic signature of the Eastern Granitoid Complex (Slavkov Terrane): $^{87}Sr/^{86}Sr_i$ = 0.704–0.705; ε_{Nd}^{i} = –1.0 to +3.0 (Finger et al. 2000a) implying a geochemically little evolved source of the granitic magmas, perhaps young calc-alkaline rocks, and/or significant mantle contribution. Worth noting in this context, however, is that the metasedimentary lithologies in this unit also show a CHUR-like isotopic signature ($^{87}Sr/^{86}Sr_i$ = 0.704–0.706; ε_{Nd}^{i} = –1.0 to +2.0; unpublished data of Finger and Pin cited by Finger et al. 2000a).

On the other hand, the Bíteš gneiss UD 2 is a typical S-type granite (see *e.g.*, high SiO_2, elevated A/CNK, thus falling into field of felsic peraluminous granites in Fig. 4c, as well as abundance of inherited zircon cores). A viable genetic model is a partial melting of a mature, ancient crustal source ($^{87}Sr/^{86}Sr_i$ = 0.7101; ε_{Nd}^{i} = –10.0). Similar ε_{Nd}^{i} values of –10 to –11, corresponding to two-stage Nd model ages (T_{Nd}^{DM}) of *c.* 2 Ga, were previously reported from analogous orthogneiss samples by Liew and Hofmann (1988) and Finger et al. (2000a).

Remarks on correlation of the Brunovistulicum s.s. and the Moravicum

The granitic magmas of the Brunovistulicum *s.s.* most likely originated from relatively immature crustal material and have little or no inherited zircon component. On the contrary, the protolith of orthogneiss from the Moravicum was derived from a more evolved continental crust rich in older detritus, especially of Mesoproterozoic and Palaeoproterozoic age. These results cast doubts on the concept that the orthogneisses of the Moravicum represent just deformed equivalents of the Brunovistulicum *s.s.* granitoid rocks (Dudek 1980; Schulmann et al. 1991, 1994). Instead, detected differences suggest that the rocks of these two units represent products of melting of distinct crustal sources with potentially different provenance. In any case, the geochemical characteristics place the magma source of all studied lithologies into an evolved continental arc setting.

However, a small number of studied samples does not allow proper description of magmatic-arc evolution that resulted in the formation of the Brunovistulian Domain rock assemblage. The age and geochemical span of the obtained data corresponds to an episodic magmatic activity observed within both ancient and modern continental magmatic-arc systems (Paterson and Ducea 2015) and to variation in chemical composition caused by continental magmatic-arc dynamics (Ducea et al. 2015).

Significance of inherited zircon age populations

Almost no inherited zircon ages were detected in the samples from the Brunovistulicum *s.s.* either due to lack of older zircons in their source(s) or the fact that they did not survive the partial melting event. The spectrum of Mesoproterozoic, Palaeoproterozoic and Neoarchean ages obtained from the zircon cores in the Bíteš orthogneiss sample UD 2 (Moravicum) could be interpreted as a recycled population of zircons from the melted source, which has been likely of sedimentary origin. The Nd model age of *c.* 2.0 Ga for the Bíteš orthogneiss UD 2 corresponds with the age spectrum obtained from inherited zircon cores of the same sample (n = 6; Fig. 9) and indicates recycling of a mainly *c*. 2 Ga old crustal component, possibly reflecting the Palaeoproterozoic (Eburnean orogenic phase of the West African Craton) event commonly described within the Moldanubian Domain (Kröner et al. 1988; Wendt et al. 1993; Friedl et al. 2004; Janoušek et al. 2010; Košler et al. 2014), its unmetamorphosed equivalent the Teplá–Barrandian Unit (Strnad and Mihaljevič 2005; Drost et al. 2007) and the Saxothuringian Domain (Linnemann and Romer 2002; Linnemann et al. 2014). This fact would suggest that the Bíteš orthogneiss nappe has been derived from the Moldanubian Domain. On the other hand, detailed provenance analysis of detrital zircons in metasedimentary rocks from the Moldanubian Domain and the Moravicum (Košler et al. 2014) indicated that the protoliths of these rocks were deposited in separate basins, yet spatially related prior to the Variscan Orogeny.

The absence of Tonian and Cryogenian ages (for a general review of zircon age spectra of the Cadomian complexes see discussion in Dörr et al. 2015) could exclude Minoan and Armorican terranes as a source area of the studied rock.

The Meso- and Palaeoproterozoic zircon cores age populations (well defined peaks between *c*. 1.2 and 2.4 Ga) from some of the metaigneous complexes in NE Austria and SW Poland (*e.g.*, Bíteš and Strzelin gneisses; Friedl et al. 2000, 2004; Oberc-Dziedzic et al. 2003; Mazur et al. 2010, 2012) are similar to our detected inherited age spectrum in the Bíteš orthogneiss (Fig. 9), and also to the previously published detrital zircon age data from the Moravicum (Košler et al. 2014). These age populations can be correlated with the orogenic events reported from the Amazonian cratonic province (Cardona et al. 2009; McLelland et al. 2010). In contrast, the abundance of gneisses derived from early Palaeozoic granitic protoliths together with lack of Mesoproterozoic and Palaeoproterozoic inheritance are considered as evidence of the North African affinity typical of the Armorican terranes (Linnemann et al. 2004, 2008; Samson et al. 2005). On this basis, the whole Brunovistulian Domain has been correlated with the South American (Avalonian) part of Gondwana (Friedl et al. 2000, 2004; Mazur et al. 2010).

However, broadly similar zircon populations from the Neoproterozoic sedimentary rocks were found also in several parts of Baltica (*e.g.*, Kuznetsov et al. 2010; Bingen et al. 2011) as well as within terranes belonging to the Trans European Suture Zone (Łysogóry and Małopolska massifs) (Valverde-Vaquero et al. 2000; Nawrocki et al. 2007). Presence of key Meso- and Palaeoproterozoic zircon ages within different continental segments (both Avalonia and Baltica) indicates that only zircon age data themselves are not useful to unequivocally distinguish the provenance of the Brunovistulian Domain. The original position of the Brunovistulian Domain during Cadomian Orogeny still remains uncertain. Further detailed geochronological studies of zircon inherited cores from magmatic rocks or detrital zircons from sedimentary rocks could shed more light on this issue.

Geotectonic implications

The new age data combined with the geochemical signatures from all the studied parts of the Brunovistulian Domain suggest their origin in the same continental arc setting.

The obtained time span of the protolith crystallization ages could mean that the continental arc-related magmas were created in course of a long-lasting Late Neoproterozoic episodic magmatic activity within the Brunovistulian Domain. Long duration of the magmatic system could have enabled an involvement of heterogeneous crustal components – as indicated by variable Nd model ages – that may have come from spatially distant domains. Such a persistent Cadomian subduction zone activity has been proposed along the whole active northern margin of the Gondwana supercontinent (period of main magmatism at *c.* 635–570 Ma; Murphy et al. 2004; Nance and Linnemann 2008).

The long-lasting widespread subduction-related magmatism has been over last 15 years reported from many Cadomian basement complexes. The presence of arc-derived clastic material in the Cadomian accretionary wedge-type sequences of the Teplá–Barrandian Unit indicates voluminous arc-related magmatic activity at *c.* 610–560 Ma (Dörr et al. 2002; Sláma et al. 2008a; Hajná et al. 2013). Detrital zircon age spectra from the Cadomian basement of the Saxothuringian Domain show arc-type magmatism in the interval of *c.* 750–570 Ma (Linnemann et al. 2014).

The long-lived Late Proterozoic magmatic arc along the northern Gondwana margin has been inferred for the Iberian Massif (Pereira et al. 2011; Albert et al. 2015a; Rubio-Ordóñez et al. 2015) and the Eastern Pyrenees (Casas et al. 2015). The Neoproterozoic arc-related magmatic activity with the time span between c. 630 and 550 Ma is also well documented in the orogenic belts of the West Gondwana not involved into younger orogens. These are for example the Dom Feliciano–Kaoko Belt (see summary in Konopásek et al. 2016), Ribeira Belt (Heilbron and Machado 2003) and the Araçuaí Belt (Tedeschi et al. 2016) today exposed along the east coast of Brazil. Moreover, the similar time interval of arc-related magmatism has been reported from the Timanides in the NE margin of Baltica (western continuation of the Cadomian orogen in Neoproterozoic; *e.g.*, Pease et al. 2004; Kuznetsov et al. 2007).The existence of Early Cambrian magmatic arc along the northern margin of East Gondwana is documented in the eastern Mediterranean region (Romano et al. 2004; Dörr et al. 2015), the Western Pontides (Şahin et al. 2014) and the Central Iranian Block (Moghadam et al. 2015).

The view that all three studied parts of the Brunovistulian Domain belonged to the same magmatic arc is, however, challenged by the presence of Mesoproterozoic to Palaeoproterozoic inherited zircon ages in the Bíteš orthogneiss, by the lack of inherited zircon ages in the Brunovistulicum *s.s*. granitoids, and by different Depleted Mantle Nd model ages of the whole-rock samples. Winchester et al. (2006) pointed out the fact that the Mesoproterozoic zircon ages obtained from the orthogneisses belong to the Moravicum, but not to the Brunovistulicum *s.s*. and suggested the possibility of former independence of the Moravicum basement from the Brunovistulicum *s.s*. Nevertheless, the lack of old zircon cores can be simply caused by rare occurrence of inheritance typical of relatively hot and less siliceous granites with I-type or mixed I/S-type affinity (Miller et al. 2003; Janoušek 2006 and references therein). This is in line with the particularly high zircon saturation temperature of 825 °C calculated for the granodiorite UD 3.

The scenario of two independent crustal segments showing continental arc magmatism would indicate existence of an oceanic suture between the Moravicum and the Brunovistulicum *s.s*. Several studies from this region nonetheless render the existence of such a large ocean basin unlikely (absence of relicts of the ocean floor-related rocks and/or evidence for HP–LT metamorphism) (Schulmann et al. 1991; Hanžl et al. 2007a). Occurrences of the metamorphosed Devonian continental and marine sedimentary rocks sandwiched between the Brunovistulicum *s.s*. and the Moravicum (Schulmann et al. 1991; Hanžl et al. 2007a) has been interpreted as remnants of small basins rather than of a subducted extensive ocean domain (Hladil et al. 1999). The Devonian lithospheric extension regime, reported by Kalvoda et al. (2008) from the Brunovistulicum *s.s*., led more likely to the development of an attenuated continental crust with narrow segments of oceanic crust in the marginal parts of the Brunovistulian Domain.

The concept that the Brunovistulicum *s.s.* and the Moravicum belonged to the same continental segment seems most likely, even though the independent provenance of both units cannot be completely excluded. Our data confirm that the Brunovistulian Domain was a part of an Andean-type active margin formed along the northern border of the Gondwana supercontinent (Fig. 11a) after its final amalgamation (Nance et al. 1991, 2002; Murphy et al. 2004). The northern Gondwana margin-derived continental fragments rifted off the supercontinent mainland (Fig. 11b) during the Cambrian–Ordovician extensional event (Murphy et al. 2006; Linnemann et al. 2008; von Raumer and Stampfli 2008; Žák et al. 2013). Position and evolution of the Brunovistulian Domain during most of the Early Palaeozoic are unclear until the regional Devonian extension (Hladil et al. 1999; Kalvoda et al. 2008) and subsequent incorporation into the Variscan collision (Schulmann et al. 2009, 2014; Štípská et al. 2015; see Fig. 11c for details).

Comparisons of age and duration of magmatic-arc activity and its possible sources in the Brunovistulian Domain with both adjacent (Teplá–Barrandian Unit and Saxothuringian Domain) and more distant (West Gondwana, NE margin of Baltica *etc.*) Cadomian basements reveal significant similarities. These findings indicate their common evolution and probable spatial relations during the Ediacaran. Moreover they underline a global importance of the widespread Neoproterozoic–Cambrian arc-related magmatic activity throughout Peri-Gondwana and Baltica terranes for a crustal growth. However, the questions of detailed evolution and mutual configuration of different Cadomian basements remain open and thus represent a challenge for future research.

Conclusions

The presence of granitic rocks in the Brunovistulian Domain with Late Proterozoic (Ediacaran) crystallization ages provides a further evidence for a long-lived, voluminous and widespread Cadomian magmatic activity at the northern margin of Gondwana. Geochemical fingerprints show that the granitic rocks of the Brunovistulicum *s.s.* and the Moravicum were formed in a continental magmatic-arc environment. The range of crystallization ages indicates episodic magmatic activity within this arc, which has been active for at least 65 Myr during

Late Proterozoic (*c.* 635–570 Ma). The whole-rock geochemical character, Sr–Nd isotopic signatures and, in the case of the Bíteš orthogneiss, abundance of zircon inheritance seem to indicate distinct crustal sources and melting conditions for each of the studied intrusions.

The parental magmas were generated by partial melting of independent segments of a continental crust characterized by variable two-stage Depleted Mantle Nd model ages (*c.* 1.3–2.0 Ga). Variability of the sources was most likely caused by different and originally distant portions of the continental crust involved into the long-lasting magmatic-arc system. Both parts of the Brunovistulian Domain (Brunovistulicum *s.s.* and the Moravicum) together with other temporally related complexes within the Variscan belt formed segments of the northern Gondwana margin until the Early Palaeozoic times, when they were rifted off during the supercontinent break-up. These Cadomian continental segments were finally amalgamated during the Early Carboniferous Variscan collision.

Acknowledgements. We are indebted to F. Veselovský for separation of zircons, V. Erban for Sr–Nd isotopic analyses, M. Racek for CL imaging and to S. Vrána for helpful discussions. We also thank A. Gerdes for editorial handling of this manuscript. The manuscript benefited from constructive reviews by G. Zulauf and one anonymous colleague. This study was supported by the Czech Science Foundation (GACR 13-16315S to P. Štípská), LK11202 programme of the Ministry of Education of the Czech Republic (to K. Schulmann), and partly also by the Academy of Sciences of the Czech Republic institutional support to the Institute of Geophysics of the CAS, v.v.i. (RVO 67985530).

Figure captions

Fig. 1 a – Position of the Bohemian Massif (BM) within Europe. b – Generalized geological map of the Bohemian Massif (modified after Franke 2000). SX: Saxothuringian Domain; TB: Teplá–Barrandian Unit; MD: Moldanubian Domain; BD: Brunovistulian Domain; SZ: Silesicum. The solid rectangle represents the studied area. c – Simplified geologic map of the Brunovistulian Domain (modified from the geologic map of the Czech Republic, 1:500,000; Cháb et al. 2007).

Fig. 2 Mutual positon of individual units within the Brunovistulian Domain in the schematic geological cross-section along the line A–B (location shown in Fig. 1). Stars indicate approximate locations of the geochemical and geochronological samples.

Fig. 3 Macro and microphotographs of studied samples from the Brunovistulian Domain. a, b – Brno Massif granodiorite UD 3; c, d – Svratka Dome metagranite UD 5; e, f – Bíteš orthogneiss UD 2.

Fig. 4 Classification diagrams for the (meta-)igneous rocks of the Brunovistulian Domain showing samples UD 2, UD 3, UD 5 and literature data (semi-transparent symbols; Souček et al. 1992; Hanžl and Melichar 1997; Hanžl et al. 2007a; Leichmann and Höck 2008). Brno Massif data do not include the A-type Hlína suite (Hönig et al. 2014). a – Multielement plot R_1–R_2 (De La Roche et al. 1980). b – Modified SiO_2 – Na_2O + K_2O (TAS; in wt. %) classification diagram proposed by Cox et al. (1979) for plutonic rocks. The discrimination boundary between the subalkaline and alkaline domains is after Irvine and Baragar (1971). c – Multielement B–A diagram (Debon and Le Fort 1983) modified by Villaseca et al. (1998). l-P: low-peraluminous, m-P: moderately peraluminous, h-P: highly peraluminous, f-P: felsic peraluminous. d – SiO_2–K_2O plot (wt. %) with the discrimination boundaries between the tholeiitic, calc-alkaline, high-K calc-alkaline and shoshonitic rocks of Peccerillo and Taylor (1976).

Fig. 5 Binary plots of silica vs. selected major- and minor-element oxides (wt. %). Data designation as in the Figure 4.

Fig. 6 Multielement diagrams for the samples of the granitic rocks from the Western Granitoid Complex of the Brno Massif, Bíteš orthogneiss from the Moravicum, and metagranites from the core of the Svratka Dome. The semi-transparent background fields are defined by the literature data from the same units (Souček et al. 1992; Hanžl and Melichar 1997; Hanžl et al. 2007a; Leichmann and Höck 2008). a – Average Upper Continental Crust (Taylor and McLennan 1995) normalized spider plot. b – Chondrite-normalized (Boynton 1984) REE patterns.

Fig. 7 Cathodoluminescence images of typical zircon grains extracted from the studied samples. Laser spots and $^{206}Pb/^{238}U$ ages with 2σ uncertainties for UD 2, UD 3 and laser rasters and $^{206}Pb/^{238}U$ ages with 2σ uncertainties for UD 5 are marked. Laser spot-size was 19 µm for UD 2 and UD 3 and 14–24 µm for UD 5.

Fig. 8 U–Pb concordia diagrams and calculated concordia ages (in blue) for magmatic zircons (LA-ICP-MS data). **a** – Brno Massif granodiorite UD 3; **b** – Svratka Dome metagranite UD 5; **c** – Bíteš orthogneiss UD 2. n – number of used analyses (more than 90% concordance)/total number of analyses.

Fig. 9 Probability density plot (bin width = 65 Ma) showing $^{206}Pb/^{238}U$ zircon ages (LA-ICP-MS data) from the Bíteš orthogneiss UD 2 from the Moravicum (ISOPLOT; Ludwig 2008).

Fig. 10 Geotectonic discrimination diagrams for the (meta-)igneous rocks of the Brunovistulian Domain. Data designation as in the Figure 4. **a** – Multielement plot Al–Fe^T + Ti–Mg of Jensen (1976) showing the calc-alkaline (CA) character of the studied rocks. TH: tholeiitic series. **b** – Th–Zr/117–Nb/16 ternary diagram (Wood 1980). N-MORB: normal-type mid-oceanic ridge basalts; E-MORB (WPT): enriched mid-oceanic ridge basalts (within-plate tholeiites); WPA: within-plate alkali basalts; CAB: calc-alkaline basalts; IAT: island-arc tholeiites. **c** – Binary plot Y–Nb (Pearce et al. 1984). ORG: Ocean Ridge Granites, VAG: Volcanic Arc Granites, syn-COLG: Collision Granites, WPG: Within Plate Granites. **d** – Binary plot Y + Nb–Rb (Pearce et al. 1984) (the same abbreviations).

Fig. 11 Schematic sketches demonstrating proposed tectonic evolution of the Brunovistulian Domain. **a** – Cadomian magmatic-arc stage at the Late Proterozoic; **b** – Early Cambrian initiation of the Gondwana margin break-up ("back-arc" position of the Letovice Complex is assumed); **c** – Variscan continental collision at the Early Carboniferous; **References**: (1) this study, (2) Kemnitz et al. (2002), (3) Linnemann et al. 2008, (4) Sláma et al. 2008a, (5) Nance et al. (2010), (6) Finger et al. (1998), (7) Mazur et al. (2012), (8) Soejono et al. (2010), (9, 10), Schulmann et al. (1991, 1994), (11) Štípská and Schulmann (1995), (12) Štípská et al. (2015).

Table captions

Table 1 Major-element whole-rock geochemical analyses (wt. %)

Table 2 Trace-element whole-rock geochemical analyses (ppm)

Table 3 Sr–Nd isotopic data

Electronic supplementary material

Laser ablation ICP-MS U–Pb zircon data

References

Albert R, Arenas R, Gerdes A, Sánchez Martínez S, Marko L (2015a) Provenance of the HP-HT subducted margin in the Variscan belt (Cabo Ortegal Complex, NW Iberian Massif). J Metamorph Geol 33:959–979

Albert R, Arenas R, Gerdes A, Sánchez Martínez S, Fernández-Suárez J, Fuenlabrada JM (2015b) Provenance of the Variscan Upper Allochthon (Cabo Ortegal Complex, NW Iberian Massif). Gondwana Res 28:1434–1448

Bandres A, Eguiluz L, Gil Ibarguchi JI, Palacios T (2002) Geodynamic evolution of a Cadomian arc region: the northern Ossa-Morena zone, Iberian Massif. Tectonophysics 352:105–120

Belka Z, Valverde-Vaquero P, Dörr W, Ahrendt H, Wemmer K, Franke W, Schäer J (2002) Accretion of first Gondwana-derived terranes at the margin of Baltica. In: Winchester JA, Pharaoh TC, Verniers J (eds) Palaeozoic Amalgamation of Central Europe. Geological Society, London, Special Publications 201:19–36

Bingen B, Belousova EA, Griffin WL (2011) Neoproterozoic recycling of the Sveconorwegian Orogenic Belt: detrital-zircon data from the Sparagmite basins in the Scandinavian Caledonides. Precambr Res 189:347–367

Boynton WV (1984) Cosmochemistry of the rare earth elements: meteorite studies. In: Henderson P (ed) Rare Earth Element Geochemistry. Elsevier, Amsterdam, 63–114

Cháb J, Stráník Z, Eliáš M (2007) Geological Map of the Czech Republic 1:500 000. Czech Geological Survey, Prague

Cardona A, Cordani UG, Ruiz J, Valencia VA, Armstrong R, Chew D, Nutman A, Sanchez AW (2009) U–Pb zircon geochronology and Nd isotopic signatures of the Pre-Mesozoic metamorphic basement of the Eastern Peruvian Andes: growth and provenance of a Late Neoproterozoic to Carboniferous accretionary orogen on the northwest margin of Gondwana. J Geol 117:285–305

Casas JM, Navidad M, Castiñeiras P, Liesa M, Aguilar C, Carreras J, Hofmann M, Gärtner A, Linnemann U (2015) The Late Neoproterozoic magmatism in the Ediacaran series of the Eastern Pyrenees: new ages and isotope geochemistry. Int J Earth Sci 104:909–925

Castiñeiras P, Navidad M, Liesa M, Carreras J, Casas JM (2008) U–Pb zircon ages (SHRIMP) for Cadomian and Early Ordovician magmatism in the Eastern Pyrenees: New insights into the pre-Variscan evolution of the northern Gondwana margin. Tectonophysics 461:228–239

Chantraine J, Egal E, Thieblemont D, Le Goff E, Guerrot C, Ballévre M, Guennoc P (2001) The Cadomian active margin (north Armorican Massif, France): a segment of the North Atlantic Pan-African belt. Tectonophysics 33:1–18

Cox KG, Bell JD, Pankhurst RJ (1979) The Interpretation of Igneous Rocks. George Allen & Unwin, London, 1–450

Dallmeyer RD, Franke W, Weber K (1995) Pre-Permian Geology of Central and Eastern Europe. Springer, Berlin, 1–593

De La Roche H, Leterrier J, Grandclaude P, Marchal M (1980) A classification of volcanic and plutonic rocks using R_1R_2-diagram and major element analyses – its relationships with current nomenclature. Chem Geol 29:183–210

Debon F, Le Fort P (1983) A chemical–mineralogical classification of common plutonic rocks and associations. Trans Roy Soc Edinb, Earth Sci 73:135–149

D'Lemos RS, Strachan RA, Topley CG (1990) The Cadomian Orogeny in the north Armorican Massif: a brief review. In: D'Lemos RS, Strachan RA, Topley CG (eds) The Cadomian Orogeny. Geological Society, London, Special Publications 51:3–12

Drost K, Romer RL, Linnemann U, Fatka O, Kraft P, Marek J (2007) Nd–Sr–Pb isotopic signatures of Neoproterozoic–Early Paleozoic siliciclastic rocks in response to changing geotectonic regimes: A case study from the Barrandian area (Bohemian Massif, Czech Republic). In: Linnemann U, Nance RD, Kraft P, Zulauf G (eds) The Evolution of the Rheic Ocean: From Avalonian–Cadomian Active Margin to Alleghenian–Variscan Collision. Geological Society of America, Special Papers 423:191–208

Drost K, Gerdes A, Jeffries T, Linnemann U, Storey C (2011) Provenance of Neoproterozoic and early Paleozoic siliciclastic rocks of the Teplá–Barrandian Unit (Bohemian Massif): Evidence from U–Pb detrital zircon ages. Gondwana Res 19:213–231

Dörr W, Fiala J, Vejnar Z, Zulauf G (1998) U–Pb zircon ages and structural development of metagranitoids of the Teplá crystalline complex: evidence for pervasive Cambrian plutonism within the Bohemian Massif (Czech Republic). Geol Rundsch 87:135–149

Dörr W, Zulauf G, Fiala J, Franke W, Vejnar Z (2002) Neoproterozoic to Early Cambrian history of an active plate margin in the Teplá–Barrandian Unit–a correlation of U–Pb isotopic-dilution-TIMS ages (Bohemia, Czech Republic). Tectonophysics 352:65–85

Dörr W, Zulauf G, Gerdes A, Lahaye Y, Kowalczyk G (2015) A hidden Tonian basement in the eastern Mediterranean: Age constraints from U–Pb data of magmatic and detrital zircons of the External Hellenides (Crete and Peloponnesus). Precambr Res 258:83–108

Dudek A (1980) The crystalline basement block of the Outer Carpathians in Moravia: BrunoVistulicum. Rozpr Čs Akad Věd 90:3–85

Dudek A, Melková J (1975) Radiometric age and isotopic data determination in the crystalline basement of the Carpathian Foredeep and of the Moravian Flysch. Věst Ústř Úst Geol 50:257–264

Ducea MN, Saleeby JB, Bergantz G (2015) The Architecture, Chemistry, and Evolution of Continental Magmatic Arcs. Annu Rev Earth Planet Sci 43:299–333

Dunstan LP, Gramlich JW, Barnes IL, Purdy WC (1980) Absolute isotopic abundance and the atomic weight of a reference sample of thallium. J Res Nat Bur Stand 85: 1–10

Fernández-Suárez J, Gutiérrez-Alonso G, Jenner GA, Tubrett MN, (2000) New ideas on the Proterozoic–Early Palaeozoic evolution of NW Iberia: insights from U–Pb detrital zircon ages. Precambr Res 102:185–206

Finger F, Pin C (1997) Arc-type crustal zoning in the Brunovistulicum, eastern Czech Republic: a trace of the late Proterozoic Euro-Gondwana margin. J Czech Geol Soc 42:53

Finger F, Frasl G, Dudek A, Jelínek E, Thöni M (1995) Igneous activity (Cadomian plutonism in the Moravo–Silesian basement). In: Dallmeyer RD, Franke W, Weber KP (eds) Pre-Permian Geology of Central and Eastern Europe. Springer-Verlag, Berlin, 495–507

Finger F, von Quadt A, Pin C, Steyrer HP (1998) The ophiolite chain along the western Moravo-Silesian plate margin – a trace of the Rheic suture? Acta Univ Carol, Geol 42:244–245

Finger F, Hanžl P, Pin C, von Quadt A, Steyrer HP (2000a) The Brunovistulian: Avalonian Precambrian sequence at the eastern end of the Central European Variscides? In: Franke W, Haak V, Oncken O, Tanner D (eds) Orogenic Processes: Quantification and Modelling in the Variscan Belt. Geological Society, London, Special Publications 179:103–112

Finger F, Tichomirowa M, Pin C, Hanžl P (2000b) Relics of early-Panafrican metabasite–metarhyolite formation in the Brno Massif, Moravia, Czech Republic. Int J Earth Sci (Geol Rundsch) 89:328–335

Finger F, Gerdes A, Janoušek V, René M, Riegler G (2007) Resolving the Variscan evolution of the Moldanubian sector of the Bohemian Massif: the significance of the Bavarian and the Moravo–Moldanubian tectonometamorphic phases. J Geosci 52:9–28

Franke W (2000) The mid-European segment of the Variscides: tectonostratigraphic units, terrane boundaries and plate tectonic evolution. In: Franke W, Haak V, Oncken O, Tanner D (eds) Orogenic Processes: Quantification and Modelling in the Variscan Belt. Geological Society, London, Special Publications 179:35–61

Friedl G, Finger F, McNaughton NJ, Fletcher IR (2000) Deducing the ancestry of terranes: SHRIMP evidence for South America-derived Gondwana fragments in central Europe. Geology 28:1035–1038

Friedl G, Finger F, Paquette JL, von Quadt A, McNaughton NJ, Fletcher IR (2004) Pre-Variscan geological events in the Austrian part of the Bohemian Massif deduced from U/Pb zircon ages. Int J Earth Sci 93:802–823

Fritz H, Dallmeyer RD, Neubauer F (1996) Thick-skinned versus thin-skinned thrusting: rheology controlled thrust propagation in the Variscan collisional belt (the southeastern Bohemian Massif, Czech Republic–Austria). Tectonics 15:13 89–1413

Gerdes A, Zeh A (2006) Combined U–Pb and Hf isotope LA-(MC-) ICP-MS analyses of detrital zircons: Comparison with SHRIMP and new constraints for the provenance and age of an Armorican metasediment in Central Germany. Earth Planet Sci Lett 249:47–61

Gürsu S, Goncuoglu MC (2008) Petrogenesis and geodynamic evolution of the Late Neoproterozoic post-collisional felsic magmatism in NE Afyon area, western central Turkey. In: Ennih N, Liégeois J-P (eds) The Boundaries of the West African Craton. Geological Society, London, Special Publications 297:409–431

Hajná J, Žák J, Kachlík V, Chadima M (2010) Subduction-driven shortening and differential exhumation in a Cadomian accretionary wedge: The Teplá-Barrandian unit, Bohemian Massif. Precambr Res 176:27–45

Hajná J, Žák J, Kachlík V, Dörr W, Gerdes A (2013) Neoproterozoic to early Cambrian Franciscan-type mélanges in the Teplá–Barrandian unit, Bohemian Massif: Evidence of modern-style accretionary processes along the Cadomian active margin of Gondwana? Precambr Res 224:653–670

Hanžl P, Melichar R (1997) The Brno Massif: a section through the active continental margin of a composed terrane? Krystalinikum 23:33–58

Hanžl P, Hrdličková K, Čtyroká J, Čurda J, Gilíková H, Gürtlerová P, Kabátník P, Kratochvílová H, Manová M, Maštera L, Neudert O, Otava J, Tomanová Petrová P, Šalanský K, Šrámek J, Švecová J, Vít J (2007a) Explanations to Geologic map of the Czech Republic 1:25,000, sheet 24-321 Tišnov. Czech Geological Survey, Prague, 1–84

Hanžl P, Janoušek V, Žáček V, Wilimský D, Aichler J, Erban V, Pudilová M, Chlupáčová M, Buriánková K, Mixa P, Pecina V (2007b) Magmatic history of granite-derived mylonites from the southern Desná Unit (Silesicum, Czech Republic). Mineral Petrol 89:45–75

Heilbron M, Machado N.(2003) Timing of terrane accretion in the Neoproterozoic–Eopaleozoic Ribeira orogen (SE Brazil). Precambr Res 125:87–112

Hladil J, Melichar R, Otava J, Galle A, Krs M, Man O, Pruner P, Čejchan P, Orel P (1999) The Devonian in the Easternmost Variscides, Moravia: a holistic analysis directed towards comprehension of the original context. Abh Geol BA 54:27–47

Höck V (1995) Moravian Zone: metamorphic evolution. In: Dallmeyer RD, Franke W, Weber K (eds) Pre-Permian Geology of Central and Eastern Europe. Springer, Berlin, 541–553

Höck V, Montag O, Leichmann J (1997) Ophiolite remnants at the eastern margin of the Bohemian Massif and their bearing on the tectonic evolution. Mineral Petrol 60:267–287

Hönig S, Čopjaková R, Škoda R, Novák M, Dolejš D, Leichmann J, Galiová-Vašínová M (2014) Garnet as a major carrier of the Y and REE in the granitic rocks: An example from the layered anorogenic granite in the Brno Batholith, Czech Republic. Amer Mineral 99:1922–1941

Horn I, Rudnick RL, McDonough WF (2000) Precise elemental and isotope ratio determination by simultaneous solution nebulization and laser ablation-ICP-MS: application to U–Pb geochronology. Chem Geol 164:281–301

Irvine TN, Baragar WRA (1971) A guide to the chemical classification of the common volcanic rocks. Can J Earth Sci 8:523–548

Jackson SE, Pearson NJ, Griffin WL, Belousova EA (2004) The application of laser ablation-inductively coupled plasma-mass spectrometry to in situ U–Pb zircon geochronology. Chem Geol 211:47–69

Jacobsen SB, Wasserburg GJ (1980) Sm–Nd isotopic evolution of chondrites. Earth Planet Sci Lett 50:139–155

Janoušek V (2006) *Saturnin,* R language script for application of accessory-mineral saturation models in igneous geochemistry. Geol Carpath 57:131–142

Janoušek V, Farrow CM, Erban V (2006) Interpretation of whole-rock geochemical data in igneous geochemistry: introducing Geochemical Data Toolkit (GCDkit). J Petrol 47:1255–1259

Janoušek V, Wiegand B, Žák J (2010) Dating the onset of Variscan crustal exhumation in the core of the Bohemian Massif: new U–Pb single zircon ages from the high-K calc-alkaline granodiorites of the Blatná suite, Central Bohemian Plutonic Complex. J Geol Soc, London 167:347–360

Jelínek E, Dudek A (1993) Geochemistry of the subsurface Precambrian plutonic rocks from the Brunovistulian Complex in the Bohemian Massif, Czechoslovakia. Precambr Res 62:103–125

Jensen LS (1976) A New Cation Plot for Classifying Subalkalic Volcanic Rocks. Ontario Geological Survey, Misc Pap 66:1–22

Kalvoda J, Melichar R, Leichmann J, Bábek O (2002) Late Proterozoic–Paleozoic tectonostratigraphic development and paleogeography of Brunovistulian Terrane and comparison with other terranes at the SE margins of Baltica–Laurussia. J Czech Geol Soc 47:3–4

Kalvoda J, Bábek O, Fatka O, Leichmann J, Melichar R, Nehyba S, Špaček P (2008) Brunovistulian Terrane (Bohemian Massif, Central Europe) from late Proterozoic to late Paleozoic: a review. Int J Earth Sci 97:497–518

Kemnitz H, Romer R, Oncken O (2002) Gondwana break-up and the northern margin of the Saxothuringian belt (Variscides of Central Europe). Int J Earth Sci 91:246–259

Konopásek J, Schulmann K, Johan V (2002) Eclogite-facies metamorphism at the eastern margin of the Bohemian Massif – subduction prior to continental underthrusting? Eur J Mineral 14:701–713

Konopásek J, Sláma J, Košler J (2016) Linking the basement geology along the Africa–South America coasts in the South Atlantic. Precambr Res 280:221–230

Košler J, Sylvester PJ (2003) Present trends and the future of zircon in geochronology: laser ablation ICP–MS. In: Hanchar JM, Hoskin PWO (eds) Zircon. Mineralogical Society of America and Geochemical Society Reviews in Mineralogy and Geochemistry 53:243–275

Košler J, Fonneland H, Sylvester PJ, Tubrett M, Pedersen RB (2002) U–Pb dating of detrital zircons for sediment provenance studies – a comparison of laser ablation ICP-MS and SIMS techniques. Chem Geol 182:605–618

Košler J, Konopásek J, Sláma J, Vrána S (2014) U–Pb zircon provenance of Moldanubian metasediments in the Bohemian Massif. J Geol Soc, London 171:83–95

Kröner A, Wendt I, Liew TC, Compston W, Todt W, Fiala J, Vaňková V, Vaněk J (1988) U–Pb zircon and Sm–Nd model ages of high-grade Moldanubian metasediments, Bohemian Massif, Czechoslovakia. Contrib Mineral Petrol 99:257–266

Kröner A, Štípská P, Schulmann K, Jaeckel P (2000) Chronological constrains on the pre-Variscan evolution of the northeastern margin of the Bohemian Massif, Czech Republic. In: Franke W, Haak V, Oncken O, Tanner D (eds) Orogenic Processes: Quantification and Modelling in the Variscan Fold Belt. Geological Society, London, Special Publications 179:175–197

Kuznetsov NB, Soboleva AA, Udoratina OV, Hertseva MV, Andreichev VL (2007) Pre-Ordovician tectonic evolution and volcano-plutonic associations of the Timanides and northern Pre-Uralides, northeast part of the East European Craton. Gondwana Res 12:05–323

Kuznetsov NB, Natapov LM, Belousova EA, O'Reilly SY, Griffin WL (2010) Geochronological, geochemical and isotopic study of detrital zircon suites from late Neoproterozoic clastic strata along the NE margin of the East European Craton: implications for plate tectonic models. Gondwana Res 17:583–601

Leichmann J, Höck V (2008) The Brno Batholith: an insight into the magmatic and metamorphic evolution of the Cadomian Brunovistulian Unit, eastern margin of the Bohemian Massif. J Geosci 53:281–305

Liew TC, Hofmann AW (1988) Precambrian crustal components, plutonic associations, plate environment of the Hercynian Fold Belt of central Europe: indications from a Nd and Sr isotopic study. Contrib Mineral Petrol 98:129–138

Linnemann U, Romer RL (2002) The Cadomian Orogeny in Saxo-Thuringia, Germany: geochemical and Nd–Sr–Pb isotopic characterization of marginal basins with constraints to geotectonic setting and provenance. Tectonophysics 352:33–64

Linnemann U, McNaughton NJ, Romer RL, Gehmlich M, Drost K, Tonk C (2004) West African provenance for Saxo-Thuringia (Bohemian Massif): Did Armorica ever leave pre-Pangean Gondwana? – U/Pb-SHRIMP zircon evidence and the Nd-isotopic record. Int J Earth Sci 93:683–705

Linnemann U, Pereira F, Jeffries TE, Drost K, Gerdes A (2008) The Cadomian Orogeny and the opening of the Rheic Ocean: the diacrony of geotectonic processes constrained by LA-ICP-MS U–Pb zircon dating (Ossa-Morena and Saxo-Thuringian zones, Iberian and Bohemian massifs). Tectonophysics 461:21–43

Linnemann U, Gerdes A, Hofmann M, Marko L (2014) The Cadomian Orogen: Neoproterozoic to Early Cambrian crustal growth and orogenic zoning along the periphery of the West African Craton–Constraints from U-Pb zircon ages and Hf isotopes (Schwarzburg Antiform, Germany). Precambr Res 244:236–278

Ludwig KR (2008) User’s Manual for Isoplot v. 3.6, a Geochronological Toolkit for Microsoft Excel. Berkeley Geochronological Center Special Publications 4:1–77

Lugmair GW, Marti K (1978) Lunar initial ^{143}Nd/^{144}Nd: differential evolution line of the lunar crust and mantle. Earth Planet Sci Lett 39:349–357

Mašek J, Zoubek J (1980) Proposal of stratigraphical terms for stratigraphical units of the Barrandian Proterozoic. Bulletin of the Czech Geological Survey 55:121–123

Matte P, Maluski H, Rajlich P, Franke W (1990) Terrane boundaries in the Bohemian Massif: result of large-scale Variscan shearing. Tectonophysics 177:151–170

Mazur S, Kröner A, Szczepański J, Turniak K, Hanžl P, Melichar R, Rodionov NV, Paderin I, Sergeev SA (2010) Single zircon U–Pb ages and geochemistry of granitoid gneisses from SW Poland: evidence for an Avalonian affinity of the Brunian microcontinent. Geol Mag 147:508–526

Mazur S, Szczepański J, Turniak K, McNaughton NJ (2012) Location of the Rheic suture in the eastern Bohemian Massif: evidence from detrital zircon data. Terra Nova 24:199–206

McLelland JM, Selleck BW, Bickford ME (2010) Review of the Proterozoic evolution of the Grenville Province, its Adirondack outlier, and the Mesoproterozoic inliers of the Appalachians. In: Tollo RP, Bartholomew MJ, Hibbard, JP, Karabinos PM (eds) From Rodinia to Pangea: The Lithotectonic Record of the Appalachian Region. Geological Society of America, Memoirs 206:21–49

Míková J, Denková P (2007) Modified chromatographic separation scheme for Sr and Nd isotope analysis in geological silicate samples. J Geosci 52:221–226

Miller CF, McDowell SM, Mapes RW (2003) Hot and cold granites? Implications of zircon saturation temperatures and preservation of inheritance. Geology 31:529–532

Moczydlowska M (1997) Proterozoic and Cambrian successions in Upper Silesia: an Avalonian Terrane in southern Poland. Geol Mag 134:679–689

Moghadam HS, Khademi M, Hu Z, Stern RJ, Santos JF, Wu Y (2015) Cadomian (Ediacaran–Cambrian) arc magmatism in the ChahJam–Biarjmand Metamorphic Complex (Iran): magmatism along the northern active margin of Gondwana. Gondwana Res 27:439–452

Murphy JB, Eguiluz L, Zulauf G (2002) Cadomian orogens, peri-Gondwanan correlatives and Laurentia–Baltica connections. Tectonophysics 352:1–9

Murphy JB, Pisarevsky SA, Nance RD, Keppie JD (2004) Neoproterozoic–Early Paleozoic evolution of peri-Gondwanan terranes: implications for Laurentia–Gondwana connections. Int J Earth Sci (Geol Rundsch) 93:659–682

Murphy JB, Gutiérrez-Alonso G, Nance RD, Fernández-Suárez J, Keppie JD, Quesada C, Strachan RA, Dostal J (2006) Origin of the Rheic Ocean: rifting along a Neoproterozoic suture? Geology 34:325–328

Nance RD, Linnemann U (2008) The Rheic Ocean: origin, evolution, and significance. GSA Today 18:4–12

Nance RD, Murphy JB, Strachan RA, D'Lemos RS, Taylor GK (1991) Late Proterozoic tectonostratigraphic evolution of the Avalonian and Cadomian terranes. Precambr Res 53:41–78

Nance RD, Murphy JB, Keppie JD (2002) A Cordilleran model for the evolution of Avalonia. Tectonophysics 352:11–31

Nance RD, Gutiérrez-Alonso G, Keppie JD, Linnemann U, Murphy JB, Quesada C, Strachan R, Woodcock NH (2010) Evolution of the Rheic Ocean. Gondwana Res 17:194–222

Nawrocki J, Żylińska A, Bula Z, Grabowski J, Krywiec P, Poprawa P (2004) Early Cambrian location and affinities of the Brunovistulian Terrane (Central Europe) in the light of palaeomagnetic data. J Geol Soc, London 161:513–522

Nawrocki J, Dunlap J, Pecskay Z, Krzemiński L, Żylińska A, Fanning M, Kozłowski W, Salwa S, Szczepanik Z, Trela W (2007) Late Neoproterozoic to Early Palaeozoic palaeogeography of the Holy Cross Mountains (Central Europe): an integrated approach. J Geol Soc, London 164:405–423

Neubauer F (2002) Evolution of late Neoproterozoic to early Paleozoic tectonic elements in Central and Southeast European Alpine mountain belts: review and synthesis. Tectonophysics 352:87–103

Oberc-Dziedzic T, Klimas K, Kryza R, Fanning CM (2003) SHRIMP zircon geochronology of the Strzelin gneiss, SW Poland: evidence for a Neoproterozoic thermal event in the Fore-Sudetic Block, Central European Variscides. Int J Earth Sci 92:701–711

Paterson SR, Ducea MN (2015) Arc Magmatic Tempos: Gathering the Evidence. Elements 11:91–98

Paton C, Woodhead, JD, Hellstrom JC, Hergt JM, Greig A, Maas R (2010) Improved laser ablation U–Pb zircon geochronology through robust downhole fractionation correction. Geochem Geophys Geosyst 11, doi: 10.1029/2009GC002618

Pearce JA, Harris NBW, Tindle AG (1984) Trace element discrimination diagrams for the tectonic interpretation of granitic rocks. J Petrol 25:956–983

Pease VL, Dovzhikova E, Beliakova L, Gee DG (2004) Late Neoproterozoic granitoid magmatism in the basement to the Pechora Basin, NW Russia: geochemical constraints indicate westward subduction beneath NE Baltica. In: Gee DG (ed) The Neoproterozoic Timanide Orogen of Eastern Baltica. Geological Society, London, Memoirs 30:75–85

Peccerillo A, Taylor SR (1976) Geochemistry of Eocene calc-alkaline volcanic rocks from the Kastamonu area, Northern Turkey. Contrib Mineral Petrol 58:63–81

Pereira MF, Chichorro M, Solá AR, Silva JB, Sánchez-García T, Bellido F (2011) Tracing the Cadomian magmatism with detrital/inherited zircon ages by in-situ U–Pb SHRIMP geochronology (Ossa-Morena Zone, SW Iberian Massif). Lithos 123:204–217

Petrus JA, Kamber BS, (2012).VizualAge: A Novel Approach to Laser Ablation ICP–MS U–Pb Geochronology Data Reduction. Geostand Geoanal Res 36, 247–270.

Pin C, Zalduegui JFS (1997) Sequential separation of light rare-earth elements, thorium and uranium by miniaturized extraction chromatography: application to isotopic analyses of silicate rocks. Anal Chim Acta 339: 79–89

Pin C, Briot D, Bassin C, Poitrasson F (1994) Concomitant separation of strontium and samarium–neodymium for isotopic analysis in silicate samples, based on specific extraction chromatography. Anal Chim Acta 298: 209–217Romano SS, Dörr W, Zulauf G

(2004) Cambrian granitoids in pre-Alpine basement of Crete (Greece): Evidence from U-Pb dating of zircon. Int J Earth Sci 93:844–859

Rubio-Ordóñez A, Gutiérrez-Alonso G, Valverde-Vaquero P, Cuesta A, Gallastegui G, Gerdes A, Cárdenes V (2015) Arc-related Ediacaran magmatism along the northern margin of Gondwana: geochronology and isotopic geochemistry from Northern Iberia. Gondwana Res 27:216–227

Samson SD, D'Lemos RS, Miller BV, Hamilton MA (2005) Neoproterozoic palaeogeography of the Cadomia and Avalon terranes: constraints from detrital zircon U–Pb ages. J Geol Soc, London 162:65–71

Shafaii Moghadam H, Khademi M, Hu Z, Stern RJ, Santos JF, Wu Y (2015) Cadomian (Ediacaran–Cambrian) arc magmatism in the ChahJam–Biarjmand Metamorphic Complex (Iran): magmatism along the northern active margin of Gondwana. Gondwana Res 27:439–452

Schaltegger U, Nägler TF, Corfu F, Maggetti M, Galetti G, Stosch H (1997) A Cambrian island arc in the Silvretta nappe: constraints from geochemistry and geochronology. Schweiz Mineral Petrograph Mitt 77:337–350

Schaltegger U, Schmitt AK, Horstwood MSA (2015) U–Th–Pb zircon geochronology by ID-TIMS, SIMS, and laser ablation ICP-MS: Recipes, interpretations, and opportunities. Chem Geol 402:89–110

Scharbert S, Batík P (1980) The age of the Thaya (Dyje) Pluton. Verh Geol B-A 1980:325–331

Schulmann K, Ledru P, Autran A, Melka R, Lardeaux JM, Urban M, Lobkowicz M (1991) Evolution of nappes in the eastern margin of the Bohemian Massif: a kinematic interpretation. Geol Rundsch 80:73–92

Schulmann K, Melka R, Lobkowicz MZ, Ledru P, Lardeaux JM, Autran A (1994) Contrasting styles of deformation during progressive nappe stacking at the southeastern margin of the Bohemian Massif (Thaya Dome). J Struct Geol 16:355–370

Schulmann K, Konopásek J, Janoušek V, Lexa O, Lardeaux JM, Edel JB, Štípská P, Ulrich S (2009) An Andean type Palaeozoic convergence in the Bohemian Massif. C R Geosci 341:266–286

Schulmann K, Lexa O, Janoušek V, Lardeaux JM, Edel JB (2014) Anatomy of a diffuse cryptic suture zone: an example from the Bohemian Massif, European Variscides. Geology 42:275–278

Schulz B, Bombach K, Pawlig S, Brätz H (2004) Neoproterozoic to Early-Palaeozoic magmatic evolution in the Gondwana-derived Austroalpine basement to the south of the Tauern Window (Eastern Alps). Int J Earth Sci 93:824–843

Sláma J, Dunkley DJ, Kachlík V, Kusiak MA (2008a) Transition from island-arc to passive setting on the continental margin of Gondwana: U–Pb zircon dating of Neoproterozoic metaconglomerates from the SE margin of the Teplá–Barrandian Unit, Bohemian Massif. Tectonophysics 461:44–59

Sláma J, Košler J, Condon DJ, Crowley JL, Gerdes A, Hanchar JM, Horstwood MSA, Morris GA, Nasdala L, Norberg N, Schaltegger U, Schoene B, Tubrett MN, Whitehouse MJ (2008b) Plešovice zircon – a new natural reference material for U–Pb and Hf isotopic microanalysis. Chem Geol 249:1–35

Soejono I, Žáčková E, Janoušek V, Machek M, Košler J (2010) Vestige of an Early Cambrian incipient oceanic crust incorporated in the Variscan orogen: Letovice Complex, Bohemian Massif. J Geol Soc, London 167:1113–1130

Souček J, Jelínek E, Bowes DR (1992) Geochemistry of gneisses of the eastern margin of the Bohemian Massif. In: Kukal Z (ed) Proceedings of the 1st International Conference on the Bohemian Massif. Czech Geological Survey, Prague, 269–285

Steiger RH, Jäger E (1977) Subcommission on Geochronology: convention on the use of decay constants in geo- and cosmochronology. Earth Planet Sci Lett 36:359–362

Strachan RA, D'Lemos RS, Dallmeyer RD (1996) Late Precambrian evolution of an active plate margin: North Armorican Massif, France. In: Nance RD, Thompson MD (eds) Avalonian and Related Peri-Gondwanan Terranes of the Circum–North Atlantic. Geological Society of America, Special Papers 304:319–332

Strnad L, Mihaljevič M (2005) Sedimentary provenance of Mid-Devonian clastic sediments in the Teplá–Barrandian Unit (Bohemian Massif): U–Pb and Pb–Pb geochronology of detrital zircons by laser ablation ICP-MS. Mineral Petrol 84:47–68

Suess FE (1912) Die moravische Fenster und ihre Beziehung zum Grundgebirge des Hohen Gesenkes. Denkschr Österr Akad Wiss Mat Naturwiss Kl 88:541–631

Suess FE (1926) Intrusionstektonik und Wandertektonik im variszischen Grundgebirge. Verlag von Gebrüder Borntraeger, Berlin, 1–268

Şahin SY, Aysal N, Güngör Y, Peytcheva I, Neubauer F (2014) Geochemistry and U–Pb zircon geochronology of metagranites in Istranca (Strandja) Zone, NW Pontides, Turkey: implications for the geodynamic evolution of Cadomian Orogeny. Gondwana Res 26:755–771

Štípská P, Schulmann K (1995) Inverted metamorphic zonation in a basement-derived nappe sequence, eastern margin of the Bohemian Massif. Geol J 30:385–413

Štípská P, Hacker BR, Racek M, Holder R, Kylander-Clark ARC, Schulmann K, Hasalová P (2015) Monazite Dating of Prograde and Retrograde P–T–d paths in the Barrovian terrane of the Thaya Window, Bohemian Massif. J Petrol 56:1007–1035

Tait JA, Bachtadse V, Franke W, Soffel HC (1997) Geodynamic evolution of the European Variscan fold belt: palaeomagnetic and geological constraints. Geol Rundsch 86:585–598

Taylor SR, McLennan SM (1995) The geochemical evolution of the continental crust. Rev Geophys 33:241–265

Tedeschi M, Novo T, Pedrosa-Soares A, Dissin I, Tassinari C, Silva LC, Gonçalves L, Alkmim F, Lana C, Figueiredo C, Dantes E, Medeiros S, De Campos C, Corrales F, Heilbron M (2016) The Ediacaran Rio Doce arc revisited (Araçuaí–Ribeira orogenic system, SE Brazil). J South Am Earth Sci 68:167–186

Ustaömer PA, Mundil R, Renne PR (2005) U/Pb and Pb/Pb zircon ages for arc-related intrusions of the Bolu Massif (W Pontides, NW Turkey): evidence for Late Precambrian (Cadomian) age. Terra Nova 17:215–223

Valverde-Vaquero P, Dörr W, Belka Z, Franke W, Wiszniewska J, Schastok J (2000) U–Pb single-grain dating of detrital zircon in the Cambrian of Central Poland: implications for Gondwana versus Baltica provenance studies. Earth Planet Sci Lett 184:225–240

van Breemen O, Aftalion M, Bowes DR, Dudek A, Mísař Z, Povondra P, Vrána S (1982) Geochronological studies of the Bohemian Massif, Czechoslovakia, and their significance in the evolution of Central Europe. Trans Roy Soc Edinb, Earth Sci 73:89–108

Vavrdová M, Mikuláš R, Nehyba S (2003) Lower Cambrian siliciclastic sediments in Southern Moravia (Czech Republic) and their paleogeographical constraints. Geol Carpath 54:67–79

Villaseca C, Barbero L, Herreros V (1998) A re-examination of the typology of peraluminous granite types in intracontinental orogenic belts. Trans Roy Soc Edinb, Earth Sci 89:113–119

von Raumer JF, Stampfli GM (2008) The birth of the Rheic Ocean – Early Palaeozoic subsidence patterns and subsequent tectonic plate scenarios. Tectonophysics 461:9–20
von Raumer JF, Stampfli GM, Borel G, Bussy F (2002) Organization of pre-Variscan basement areas at the north-Gondwanan margin. Int J Earth Sci 91:35–52
Wasserburg GJ, Jacobsen SB, DePaolo DJ, McCulloch MT, Wen T (1981) Precise determination of Sm/Nd ratios, Sm and Nd isotopic abundances in standard solutions. Geochim Cosmochim Acta 45:2311–2324
Watson EB, Harrison TM (1983) Zircon saturation revisited: temperature and composition effects in a variety of crustal magma types. Earth Planet Sci Lett 64:295–304
Wendt JI, Kröner A, Fiala J, Todt W (1993) Evidence from zircon dating for existence of approximately 2.1 Ga old crystalline basement in southern Bohemia, Czech Republic. Geol Rundsch 82:42–50
Wiedenbeck M, Allé P, Corfu F, Griffin WL, Meier M, Oberli F, von Quadt A, Roddick JC, Spiegel W (1995) Three natural zircon standards for U–Th–Pb, Lu–Hf, trace element and REE analyses. Geostand Newsl 19:1–23
Winchester J, Pharaoh T, Verniers J (2002) Palaeozoic amalgamation of Central Europe: an introduction and synthesis of new results from recent geological and geophysical investigations. In: Winchester JA, Pharaoh TC, Verniers J (eds) Palaeozoic Amalgamation of Central Europe. Geological Society, London, Special Publications 201:1–18
Winchester JA, Pharaoh TC, Verniers J, Ioane D, Seghedi A (2006) Palaeozoic accretion of Gondwana-derived terranes to the East European Craton: recognition of detached terrane fragments dispersed after collision with promontories. In: Gee DG, Stephenson RA (eds) European Lithosphere Dynamics. Geological Society London, Memoirs 32:323–332
Wood DA (1980) The application of a Th–Hf–Ta diagram to problems of tectonomagmatic classification and to establishing the nature of crustal contamination of basaltic lavas of the British Tertiary volcanic province. Earth Planet Sci Lett 50:11–30
Zulauf G, Dörr W, Fiala J, Vejnar Z, Dörr W, Fiala J, Vejnar Z (1997) Late Cadomian crustal tilting and Cambrian transtension in the Teplá–Barrandian unit (Bohemian Massif, Central European Variscides). Geol Rundsch 86:571–584
Žák J, Kraft P, Hajná J (2013) Timing, styles, and kinematics of Cambro–Ordovician extension in the Teplá–Barrandian Unit, Bohemian Massif, and its bearing on the opening of the Rheic Ocean. Int J Earth Sci 102:415–433

Figure

Click here to download Figure Fig 1.eps

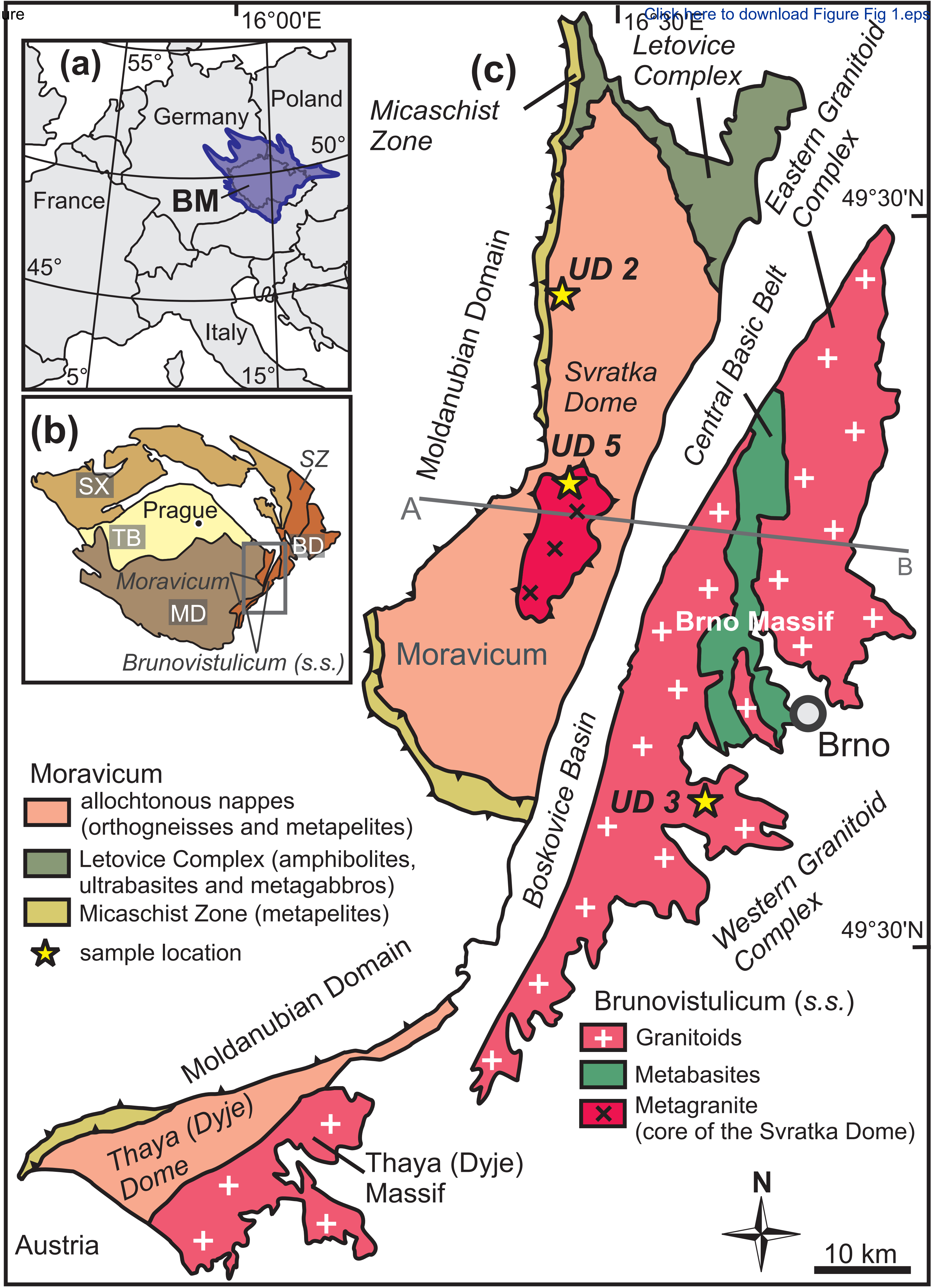

Figure

Click here to download Figure Fig 2.eps

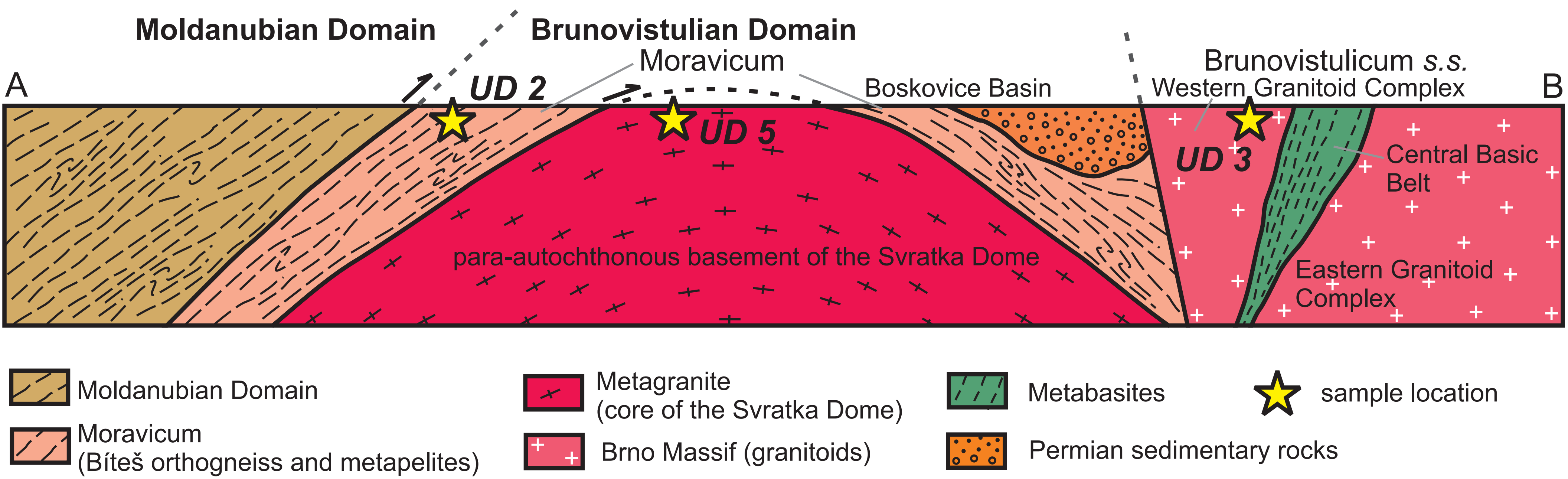

Figure

Click here to download Figure Fig 3.tif

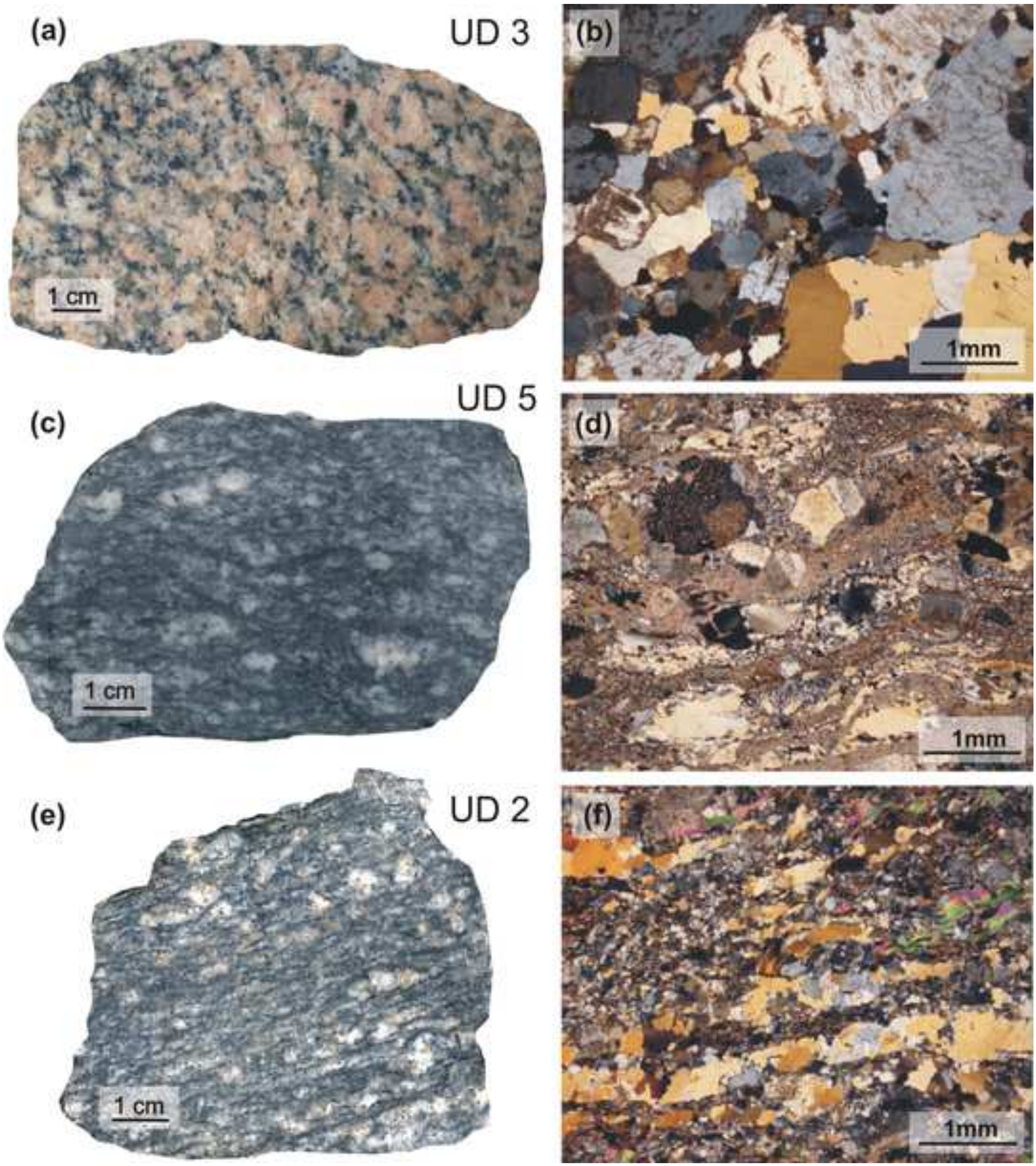

Figure

Click here to download Figure Fig 4.eps

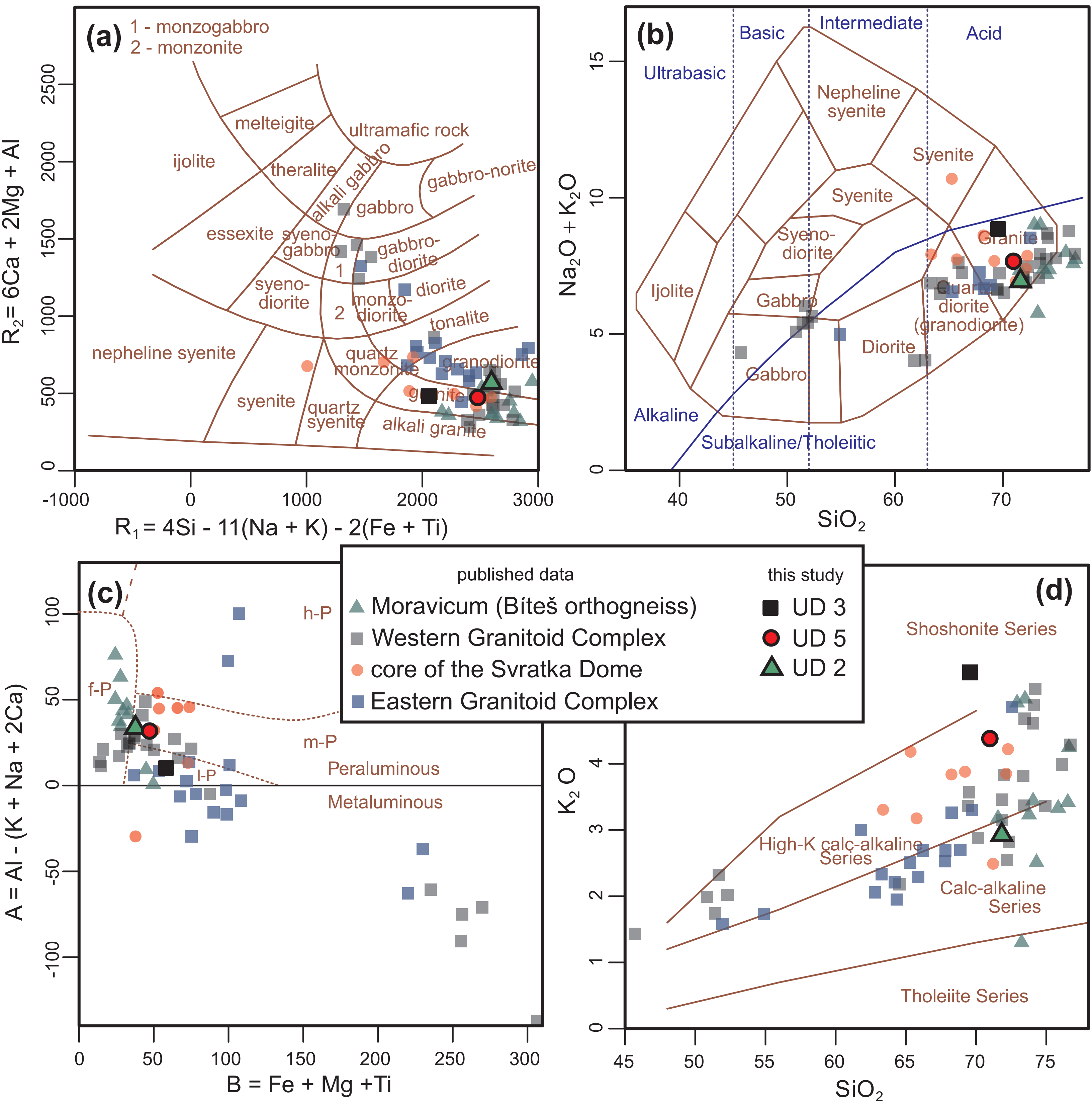

Figure

Click here to download Figure Fig 5.eps

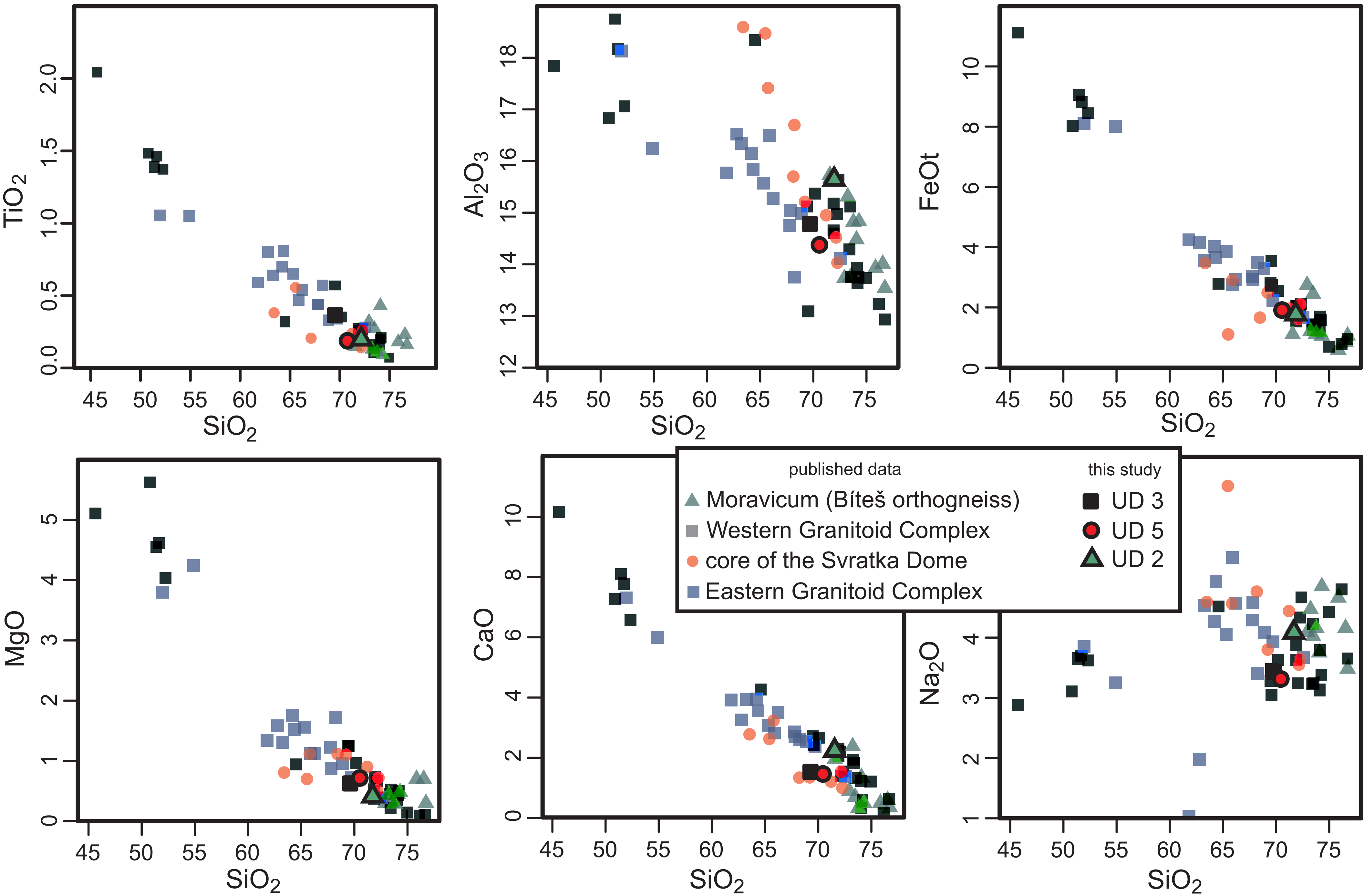

Figure

Click here to download Figure Fig 6.tif

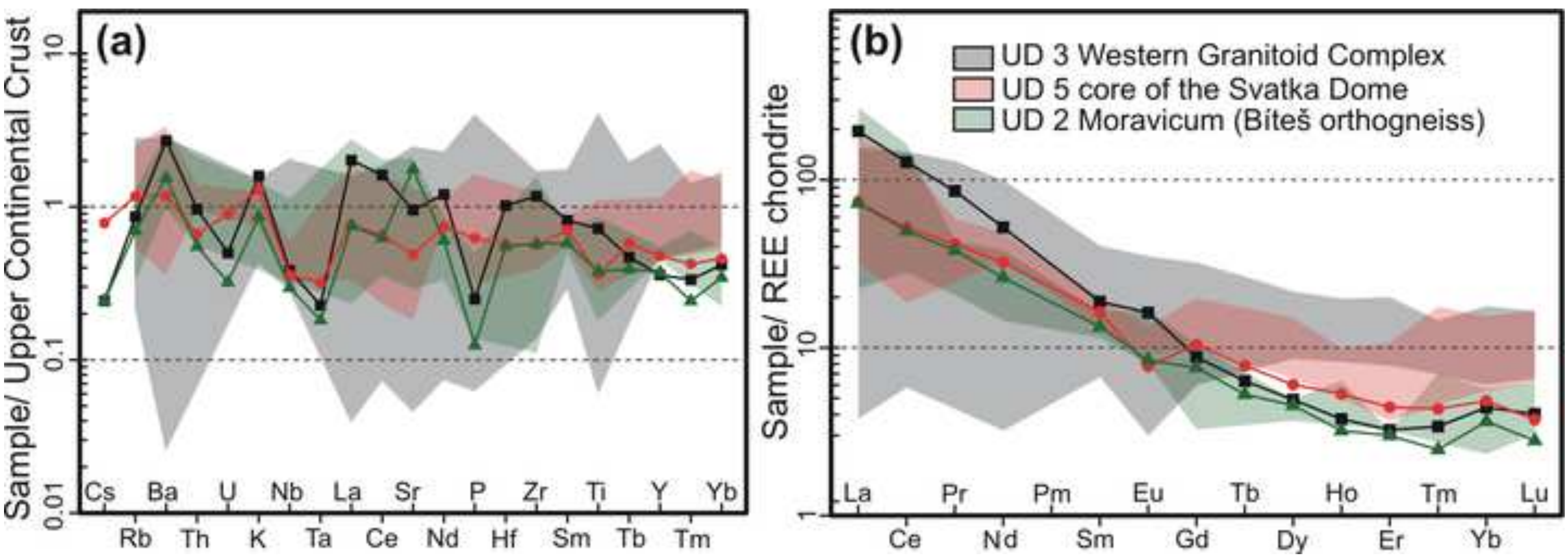

Figure

Click here to download Figure Fig 7.tif

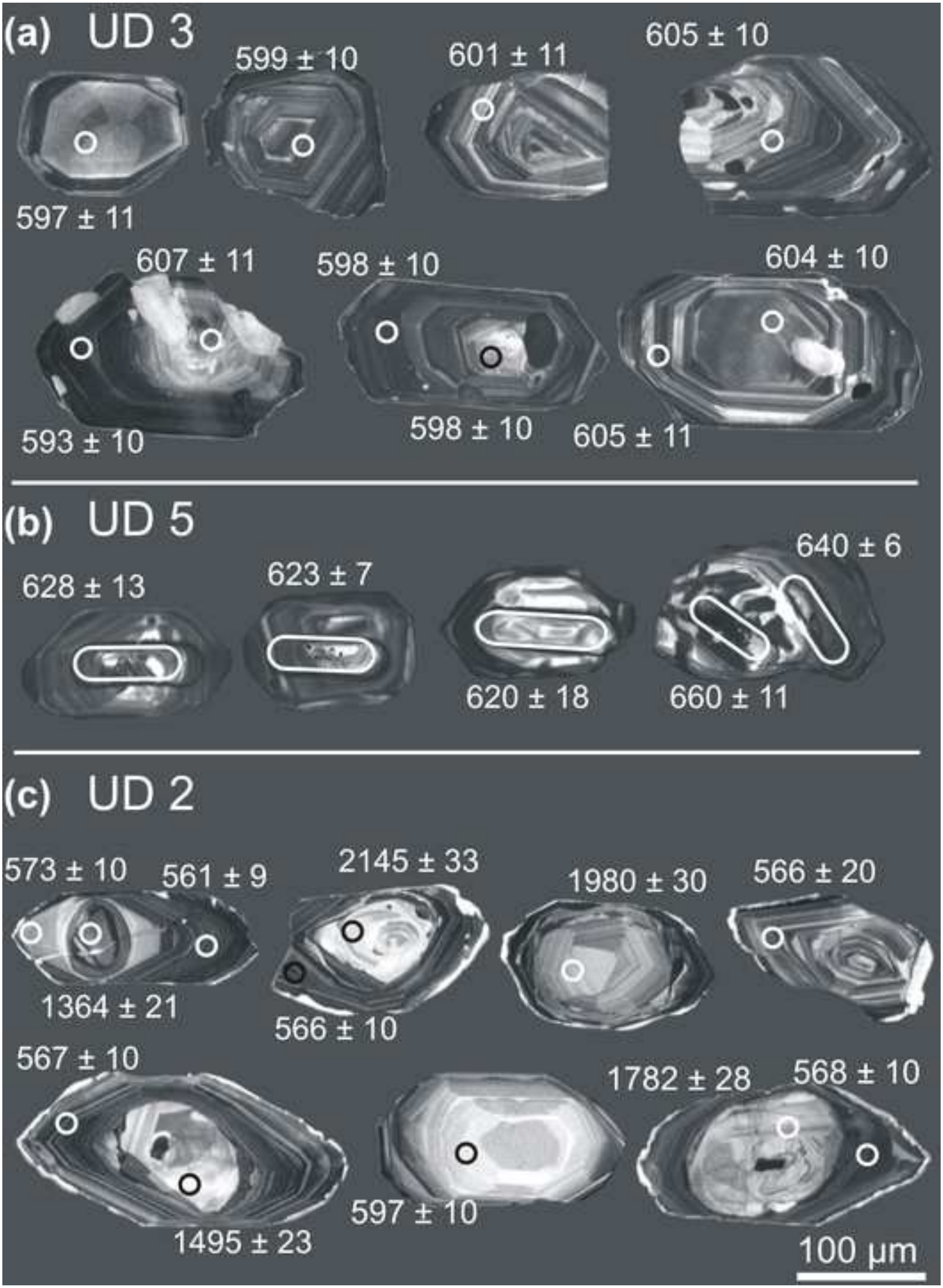

Figure

Click here to download Figure Fig 8.eps

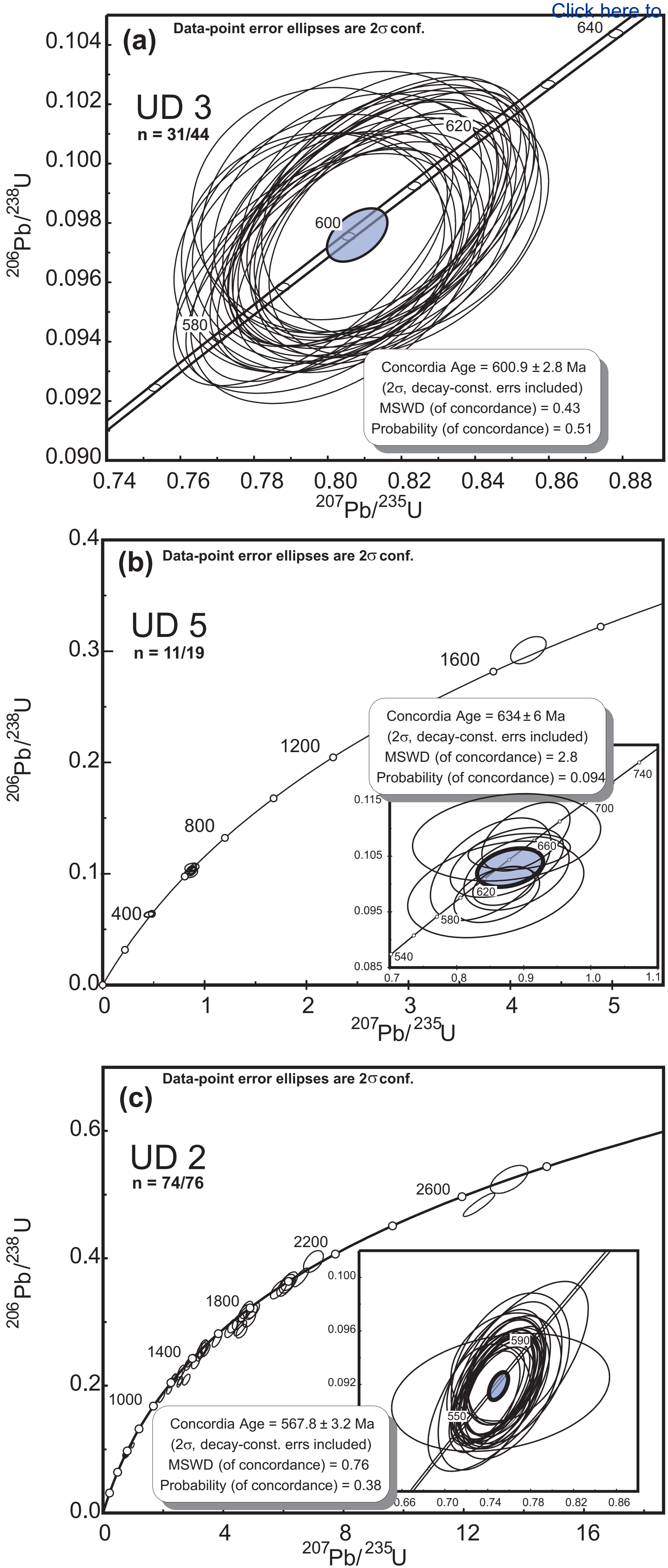

Figure

Click here to download Figure Fig 9.eps

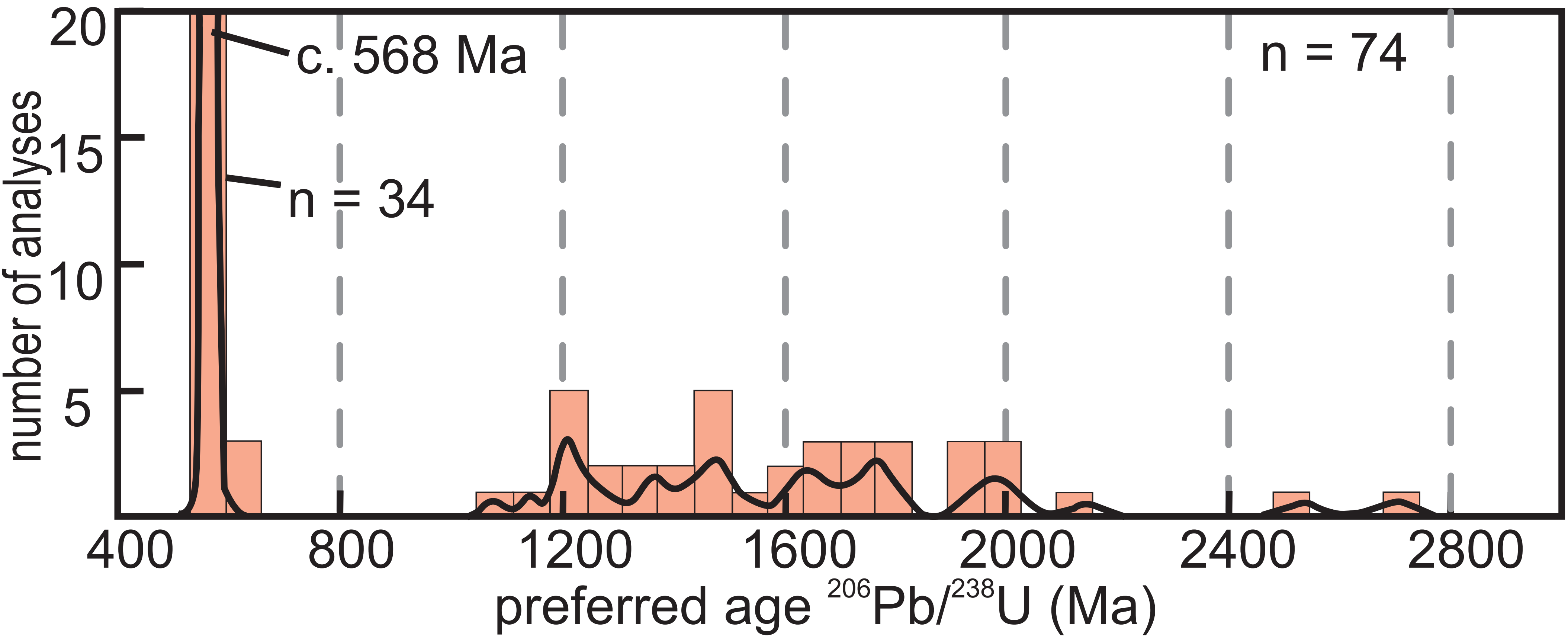

Figure

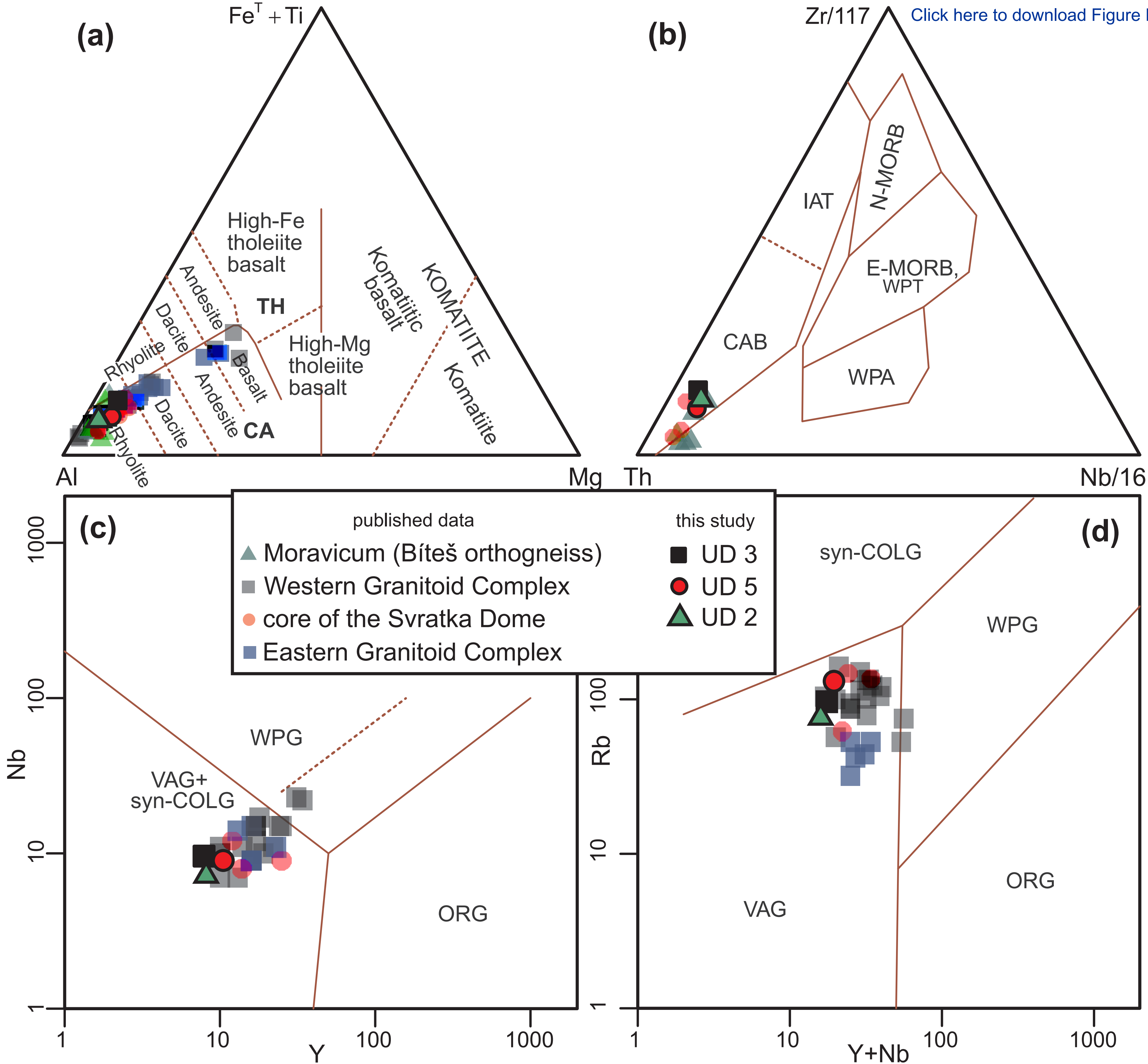

(a)
Fe^T + Ti
High-Fe tholeiite basalt
TH
High-Mg tholeiite basalt
Andesite
Dacite
Rhyolite
Basalt
CA
Komatiitic basalt
KOMATIITE
Komatiite
Al
Mg
(b)
Zr/117
IAT
N-MORB
E-MORB, WPT
CAB
WPA
Th
Nb/16
(c)
Nb
Y
WPG
VAG+ syn-COLG
ORG
(d)
Rb
Y+Nb
syn-COLG
WPG
VAG
ORG
published data
Moravicum (Býteš orthogneiss)
Western Granitoid Complex
core of the Svratka Dome
Eastern Granitoid Complex
this study
UD 3
UD 5
UD 2
1
10
100
1000

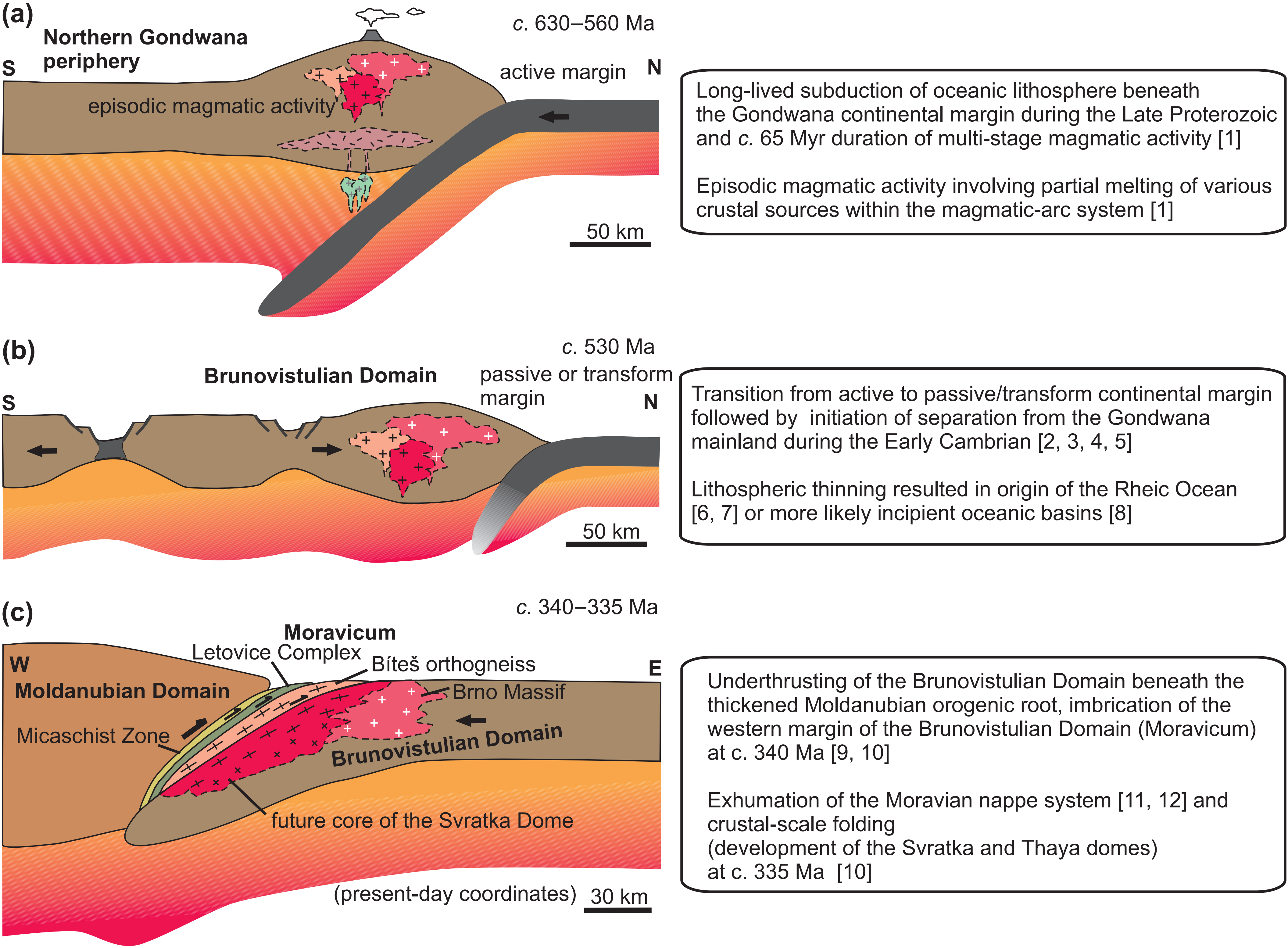
(a)
Northern Gondwana periphery
c. 630–560 Ma
S
active margin
N
episodic magmatic activity
50 km
Long-lived subduction of oceanic lithosphere beneath the Gondwana continental margin during the Late Proterozoic and c. 65 Myr duration of multi-stage magmatic activity [1]
Episodic magmatic activity involving partial melting of various crustal sources within the magmatic-arc system [1]
(b)
c. 530 Ma
Brunovistulian Domain
passive or transform margin
S
N
50 km
Transition from active to passive/transform continental margin followed by initiation of separation from the Gondwana mainland during the Early Cambrian [2, 3, 4, 5]
Lithospheric thinning resulted in origin of the Rheic Ocean [6, 7] or more likely incipient oceanic basins [8]
(c)
c. 340–335 Ma
Moravicum
Letovice Complex
Bíteš orthogneiss
W
E
Moldanubian Domain
Brno Massif
Micaschist Zone
Brunovistulian Domain
future core of the Svratka Dome
(present-day coordinates)
30 km
Underthrusting of the Brunovistulian Domain beneath the thickened Moldanubian orogenic root, imbrication of the western margin of the Brunovistulian Domain (Moravicum) at c. 340 Ma [9, 10]
Exhumation of the Moravian nappe system [11, 12] and crustal-scale folding
(development of the Svratka and Thaya domes)
at c. 335 Ma [10]

Table

Table 1 Major-element data (wt. %)

	UD 3	UD 5	UD 2
SiO_2	69.57	70.98	71.64
TiO_2	0.36	0.18	0.19
Al_2O_3	14.78	14.40	15.66
FeOt	2.74	1.87	1.77
MnO	0.06	0.07	0.04
MgO	0.63	0.68	0.43
CaO	1.50	1.47	2.26
Na_2O	3.47	3.29	4.06
K_2O	5.38	4.38	2.90
P_2O_5	0.04	0.10	0.02
LOI	0.9	2.2	0.6
Σ	99.43	99.62	99.57
K_2O/Na_2O	1.55	1.33	0.71
A/CNK	1.04	1.12	1.12
mg	29.11	39.31	30.19

Table

Table 2 Trace-element data (ppm)

	UD 3	UD 5	UD 2
Rb	96.5	131.0	78.1
Cs	0.9	2.9	0.9
Ba	1486.0	647.0	851.0
Sr	333.3	170.1	616.4
Th	10.3	7.1	5.9
U	1.4	2.5	0.9
Zr	222.8	107.0	108.8
Hf	5.9	3.3	3.2
Nb	9.6	9.0	7.4
Ta	0.5	0.7	0.4
Sc	3	3	2
Ni	5.2	2.3	1.8
Co	2.8	1.9	1.8
Pb	5.9	7.4	3.1
Zn	31	36	39
Cu	1.2	1.8	0.9
Y	7.9	10.5	8.2
La	60.4	22.9	22.5
Ce	103.2	41.9	40.1
Pr	10.47	5.07	4.65
Nd	31.3	19.3	15.7
Sm	3.67	3.18	2.60
Eu	1.19	0.57	0.62
Gd	2.28	2.70	1.97
Tb	0.30	0.37	0.25
Dy	1.58	1.94	1.46
Ho	0.27	0.38	0.23
Er	0.68	0.93	0.63
Tm	0.11	0.14	0.08
Yb	0.92	1.01	0.76
Lu	0.13	0.12	0.09
La_N/Yb_N	44.3	15.3	20.0
La_N/Sm_N	10.4	4.5	5.4
Eu/Eu*	1.26	0.59	0.84
Yb_N	4.4	4.8	3.6

Table

Table 3 Sr–Nd isotopic data

Sample	Age	$^{87}Rb/^{86}Sr$	$^{87}Sr/^{86}Sr$	2s_Sr	$^{87}Sr/^{86}Sr_i$	$^{147}Sm/^{144}Nd$	$^{143}Nd/^{144}Nd$	2s_Nd	$^{143}Nd/^{144}Nd_i$	εNd_i	$T_{Nd}DM$ 2stg
UD 3	601	0.8383	0.711957	0.000006	0.704772	0.0709	0.512093	0.000009	0.511814	-1.0	1.33
UD 5	634	2.2329	0.725420	0.000014	0.705227	0.0996	0.512043	0.000011	0.511629	-3.7	1.57
UD 2	568	0.3669	0.713056	0.000011	0.710085	0.1001	0.511765	0.000012	0.511392	-10.0	2.01

[1] subscripts 1 indicate age-corrected isotopic ratios

[2] two-stage Nd model ages (Ga) (Liew and Hofmann 1988)